TRIBHUVAN UNIVERSITY

INSTITUTE OF ENGINEERING

PULCHOWK CAMPUS

THESIS NO: 078MSPSE004

Signal Spectrum Based Condition Monitoring of Electrical Machines Based on Low Sampling Rate

by

Ashish Paudel

A THESIS

SUBMITTED TO THE DEPARTMENT OF ELECTRICAL ENGINEERING IN PARTIAL FULFILLMENT OF THE REQUIREMENT FOR THE DEGREE OF MASTER OF SCIENCE IN POWER SYSTEM ENGINEERING

DEPARTMENT OF ELECTRICAL ENGINEERING

LALITPUR, NEPAL

June 2024

COPYRIGHT

Accredited by University Grants Commission (UGC) Nepal 2020

त्रिभुवन विश्वविद्यालय
TRIBHUVAN UNIVERSITY
इन्जिनियरिङ्ग अध्ययन संस्थान
INSTITUTE OF ENGINEERING
पुल्चोक क्याम्पस
PULCHOWK CAMPUS
DEPARTMENT OF ELECTRICAL ENGINEERING
Pulchowk, Lalitpur

CERTIFICATE OF APPROVAL

The undersigned certify that they have read and recommended to the Institute of Engineering for acceptance, a dissertation entitled "**Signal Spectrum Based Condition Monitoring of Electrical Machines Based on Low Sampling Rate** ", submitted by **Ashish Paudel** in partial fulfillment of the requirement for the award of the degree of **Master of Science in Power System Engineering**.

Prof. Dr. Nava Raj Karki
Supervisor
M.Sc. in Power System Engineering

Assoc. Prof. Dr. Basanta K. Gautam
Supervisor
M.Sc. in Power System Engineering

Prof. Dr. Rajesh Karki
External Examiner
University of Saskatchewan, Canada

Assoc. Prof. Dr. Basanta K. Gautam
Program Coordinator
M.Sc. in Power System Engineering

Asst. Prof. Yuba Raj Adhikari
Head of Department
Department of Electrical Engineering

June, 2024

ABSTRACT

In the pursuit of enhancing condition monitoring techniques for electrical machines, this research addresses the intricate challenge of sampling rates in data acquisition. Conventional high-frequency sampling, while providing rich data, incurs substantial costs in memory, processing power, and computational time. Additionally, it introduces complexities related to data loss during acquisition setup. Aiming for a more balanced approach, this study explores the potential of low sampling rates, acknowledging the trade-offs in signal resolution. An innovative algorithm is proposed to harness the advantages of low sampling rates, circumventing the pitfalls of spectral leakages that often plague signal analysis. Notably, the proposed methodology eliminates the need for windowing functions, a traditional requirement in spectral analysis. The intricate process of window selection, crucial for narrowing the main lobe and reducing leakage energy, necessitates specialized knowledge. The proposed algorithm simplifies this aspect, presenting an effective solution without compromising analytical precision. This study investigates the feasibility and effectiveness of using a low sampling rate of 2 kHz for the condition monitoring of electrical machines, specifically targeting the detection of broken rotor bars (BRBs). The reduced sampling rate offers significant advantages, such as reduced data loss, lower memory requirements, and less computational burden, making it highly suitable for real-time analysis. We conducted a comparative analysis between two signal processing techniques: Fast Fourier Transform (FFT) with Hann Window and FFT after applying the Integral Number of Cycles (INOC) algorithm. Our results showed that FFT after INOC provides consistent and sharp spectral representations without the need for windowing techniques, making it a practical and efficient choice for real-time condition monitoring. The study analyzed fault harmonics across various loading conditions. Findings indicate that as the number of broken rotor bars increases, the amplitude of the fault harmonics also increases. Moreover, the difference between healthy and faulty conditions becomes more pronounced with higher loads.

Keywords: Induction Motor, Fault Diagnosis, Condition Monitoring, Broken Rotor Bar, Fourier Transform.

ACKNOWLEDGEMENT

I would like to express my heartfelt appreciation to the Capacity Enhancement in Electrical Equipment Condition Monitoring and Fault Diagnosis (CEEECoM) project, co-funded by the Erasmus+ program of the European Union. This project has provided me with a unique opportunity to conduct research on **"Signal Spectrum-Based Condition Monitoring of Electrical Machines Based on Low Sampling Rate."** I am sincerely grateful for the support and resources afforded to me through this initiative.

My gratitude extends to my esteemed supervisors**, Prof. Dr. Nava Raj Karki** and **Associate Prof. Dr. Basanta Kumar Gautam**, for their outstanding guidance, invaluable insights, and unwavering encouragement throughout the progression of this research endeavor. I would also like to thank the rest of faculty members of Department of Electrical Engineering, for their valuable input and for taking the time to review my thesis.

I would also like to express my thanks to the Department of Electrical Engineering and Automation at Aalto University, Finland and to **Prof. Anouar Belahcen** and **Nada El Bouharrouti** who have been instrumental in providing precious suggestions and generous support during the course of this research.

Last but not least, I would like to express my deepest appreciation to my family, my brothers and to my parents for their never-ending love and constant support.

Ashish Paudel
078MSPSE004
June, 2024

PREFACE

This thesis was conducted as part of student mobility program support provided under the Capacity Enhancement in Electrical Equipment Condition Monitoring and Fault Diagnosis (CEEECoM) project, co-funded by the Erasmus+ program of the European Union. This initiative has provided the necessary resources, support, and opportunities crucial for successfully completing this work.

TABLE OF CONTENTS

LIST OF FIGURES

LIST OF TABLES

ABBREVIATIONS

AI	Artificial Intelligence
BRB	Broken rotor bar
DNN	Deep Neural Network
DWT	Discrete Wavelet Transform
EMD	Empirical Mode Decomposition
FEM	Finite Element Method
FFT	Fast Fourier Transform
GA	Genetic Algorithm
IIR	Infinite Impulse Response
IM	Induction Motor
INOC	Integral Number of Cycle
IoT	Internet of Things
KNN	K-nearest neighbors
LSB	Left Side Band
MCSA	Motor Current Signature Analysis
PCA	Principle Component Analysis
PM	Predictive Maintenance
PVA	Park's Vector Analysis
RSB	Ride Side Band
SOM	Self-Organizing Maps
STFT	Short Time Fourier Transform
SVM	Support Vector Machine
WT	Wavelet Transform

CHAPTER ONE: INTRODUCTION

1.1. Electrical Machine

Electrical machines play a crucial role in nearly every sector of industrial and household activities. They serve as the backbone in various applications, including but not limited to fans, pumps, washing machines, traction, textile mills, process industries, ship thrust systems, robots, conveyor belts, and electricity generators [1]. It's important for them to work well in terms of power, speed, efficiency, reliability, and cost. They should also handle changing loads without affecting power quality too much and be easy to control.

1.2. Condition monitoring and fault diagnostic

Because machines have moving parts, they can sometimes break. Induction motors often develop issues over time, so it's important to catch these problems early to prevent serious breakdowns. If a motor fails, it can impact how well it works, the cost of running it, and even the motor's overall lifespan. As machines are used a lot in tough conditions with heavy loads, they gradually wear out and can develop problems. If they unexpectedly break down, it can cause long periods of inactivity, delays in production, safety issues, and big financial losses. To avoid these problems, condition monitoring is used as a powerful tool to make rotating machines more reliable and effective. Electrical machines can have faults, and these faults can lead to other issues. The faults can come from inside the machine, outside factors, or environmental conditions. Internal faults can be sorted based on where they originated.

We can categorize internal faults based on where they occur: either in the stator or the rotor. According to [1], typical faults in the rotor of induction motors include:

1) Bearing failure;
2) Rotor broken bars;
3) Rotor body failure;
4) Bearing misalignment;
5) Rotor misalignment;
6) Bearing loss of lubrication;
7) Rotor mechanical or thermal unbalanced;

And common faults become apparent in stator as categorized in [1]are:

1) Vibration in the frame

2) Ground faults in the stator
3) Insulation damage
4) Turn-to-turn faults in the stator
5) Phase-to-phase faults in the stator
6) Conductor displacement
7) Electrical connection failures

1.2.1. Introduction of Condition Monitoring

To make sure machines keep working well, we use a proactive method called condition monitoring. This means regularly watching, checking, and studying machines to catch any possible problems or changes in how they work. Condition monitoring is crucial because it helps us understand if machines are healthy, performing well, or starting to wear out. We do this by using sensors to collect data and advanced computer programs to analyze it. This way, maintenance teams can spot issues early, fix them quickly, and plan the best ways to keep everything running smoothly. It involves looking at how each part of the machine works, using special equipment, and studying data to predict how things might change over time [2].

1.2.2. Need of Condition Monitoring

There are numerous faults that can threaten the reliability of electrical machines, often starting as minor deviations from normal conditions. The issue with these faults is that if not addressed early on, they can escalate into severe problems. One potential solution for early fault detection in electrical machines is condition monitoring, which serves various purposes, including:

- Preventing catastrophic failures and extensive machine damage.
- Preventing loss of life, environmental damage, and economic losses
- Preventing unplanned shutdowns.
- Optimizing machine performance.
- Reducing repair time and spare parts inventory.
- Extending the maintenance cycle.
- Lowering costs and raw material usage.
- Enhancing product quality.

Condition monitoring for diagnostic purposes may involve observing various features such as vibration, noise, heat, power consumption, displacement, rotation speed, and

different electric parameters (like voltage, current, frequency, resistance, etc.). The possibilities are extensive and continue to expand, making condition monitoring applicable across diverse industries [2].

1.2.3. What and when to monitor

The selection of parameters to monitor and the frequency of monitoring depend on several factors, including the type of machine, its critical components, operating conditions, and the specific requirements of the industry or application. The conclusion is that while monitoring is easily applicable to some machines, in other situations, careful consideration is required before making a choice. However, one must always be aware of the size of the maintenance burden and avoid being persuaded to make false savings because "nothing has gone wrong so far." On the other hand, one must take into account the complexity of the monitoring system and the cost of ongoing maintenance. Nothing could be worse than spending money on sophisticated monitoring equipment that, due to poor design or upkeep, generates a large number of false alarms and is ignored [3].

When to monitor is a simpler question to resolve. When it is financially advantageous to do so or when there are paramount safety considerations to be observed, monitoring should be done. Cost-effectiveness evaluation can be a challenging process. However, in general, monitoring is beneficial when its use results in higher net annual savings. The difference between the gross annual saving and the annual costs is the net annual saving. The initial investigation, purchase, and installation fees, the staff training expenses, and the costs related to the data acquisition are all included in the cost of monitoring. This cost can be deducted from the savings accumulated over the monitoring system's lifetime [3].

1.3. Problem Statement

In the era of Industry 4.0, predictive maintenance is gaining increased significance compared to preventive or reactive maintenance. Unlike preventive or reactive approaches, predictive maintenance involves monitoring the behavior of an electrical machine to detect potential issues before they occur. This allows for timely servicing, significantly reducing system downtime and, consequently, lowering maintenance costs.

In recent decades, various traditional methods for monitoring the condition of machines

have been discussed in literature, such as motor current signature analysis (MCSA), thermal analysis, and vibration analysis. Despite being well-established, compatible with various signal-processing methods, and requiring fewer computer resources, these techniques have several drawbacks. The main issues include the use of expensive sensors, especially in thermal analysis, and difficulties in accurately identifying faulty frequency components in the early stages, particularly in MCSA-based methods. Additionally, these techniques rely on various limitations such as the structure of the machine, the environment in industrial settings, external noise, poor connection to the load, weak foundation, and the influence of the drive controller [4]. Many have used the fast Fourier techniques (FFT) for the spectral analysis but the most confound problem of FFT is its spectral leakage of the fundamental component [5].

To tackle against those problems and to improve the reliability of diagnostic algorithm, artificial intelligence (AI) based techniques with advanced mode can give promising results. Almost all AI-based diagnostic techniques necessitate a large number of data samples collected under a variety of conditions. Signals under healthy, faulty, loaded, and no-load conditions are examples of these conditions. Furthermore, different types of faults with varying severity levels under a variety of loading conditions can be used to better train advanced AI-based techniques. Because different fault types are displayed in the frequency spectrum of the motor current, it is important to have a high enough sampling frequency to collect adequate data for all possible faults scenarios. To distinguish between the fundamental frequency and closely related interharmonics, the measurement duration must also be increased. As such, using high sampling frequencies requires a sizable amount of memory to store the gathered data and a powerful processor to handle the big information. This thus drives up the measurement process's overall cost [6]. Also the computational time required is large and the data loss is also another major problem during data acquisition set up. It also increases the computation time and complexity. One of the method to mitigate the above problem is getting the data at low sampling rate but low sampling rate has also disadvantages like spectral leakages as the resolution of the signal is most important in signal analysis

So this research would attempt to mitigate problem associated with the large data acquisition by signal spectrum based condition monitoring using low sampling rate and also improve the resolution of frequency spectrum using proposed method.

1.4. Objectives

Objectives of the proposed research are illustrated with what follows.

Main Objective

To propose the algorithm for signal spectrum based condition monitoring of electrical machine based on low sampling rate without compromising the resolution of the signal.

Specific objectives

- To propose and implement a signal spectrum-based condition monitoring approach using a lower sampling rate to reduce memory requirements and overall measurement costs of the data acquisition system.
- To address also the challenges of Fast Fourier Transform (FFT) like spectral leakages and need of windowing function.
- To investigate the methodology using different loading condition of the induction motor for broken rotor bars faults.

1.5. Scope

- Low Sampling Rate Analysis: Compare the advantages of low sampling rates against traditional high-frequency sampling, focusing on memory requirements, data loss, and computational efficiency.
- Algorithm Development. Develop and validate an innovative algorithm that eliminates the need for windowing techniques in spectral analysis. Ensure the algorithm provides accurate frequency and amplitude representations without compromising analytical precision.
- Comparative Analysis: Perform a detailed comparative analysis between FFT with Hann Window and FFT purposed algorithm. Evaluate the consistency, sharpness, and reliability of the spectral representations provided by both methods.
- Loading Condition Impact Analyze the effect of different loading conditions on fault harmonics detection. Explore the relationship between loading conditions and the amplitude of fault harmonics for various BRB scenarios.
- Practical Applications: Demonstrate the practical advantages of low sampling rate data acquisition in real-time condition monitoring. Highlight the reduced memory requirements, lower computational burden, and efficiency for industrial

applications.

1.6. Limitations of the thesis

- Validated mainly on broken rotor bar faults of induction motor; needs testing on other faults and machines.
- Comparative Benchmarking: Lacks comparison with other advanced signal processing techniques.
- No Load Condition Detection: Difficulty in distinguishing fault harmonics at no load due to low slip.
- Real-time Implementation: Computational complexity needs further validation for real-world industrial use.

CHAPTER TWO: LITERATURE REVIEW

In Literature Review the various existing techniques of condition monitoring of electrical machine and signal processing techniques along with ongoing research and development of various scholars have been briefly reviewed. In recent decades, interest and research in signal analysis, fault detection, condition monitoring, and diagnosing electrical machines have steadily grown.

Detecting faults in electrical machines during their early stages is crucial to prevent severe issues that could lead to complete process failure and significant financial losses. Various fault diagnostic methods found in the literature can be broadly grouped into the following categories:

- Analyzing the current, for instance, using motor current signature analysis (MCSA).
- Studying vibrations.
- Analyzing thermal patterns.
- Assessing acoustics.
- Inferring information from the electromagnetic field.
- Detecting stray flux.

Nearly all advanced condition-monitoring techniques rely, either directly or indirectly, on these methods.

In [7] Mohamed Benbouzid provides a comprehensive list of books, workshops, conferences, and journal papers related to induction motors faults detection and diagnosis developed up to 1999. In this article the author has provided around 360 references in chronological order (from the end of the 70's up to 1999). which are divided three groups. The first group contains the information on books. The second and third one list workshops, conference, and journal papers.

2.1. Electrical and Electromagnetic Analysis

Some of the electrical faulty condition symptoms are motor current signature, voltage, flux, power and so on. Probable faults can be detected by comparison between electrical signals in healthy and unknown conditions.

Akin and colleagues [8] suggest that the reference frame theory is effective for quickly identifying faults in electric machinery systems, even in less-than-ideal situations like

offsets or imbalances. The main concept involves transforming the fault signature into a direct current (dc) quantity. By calculating the average of the signal in the fault reference frame, the remaining signal harmonics, or alternating current (ac) components, can be filtered out. This eliminates the need for additional filters like notch or low-pass filters to remove the fundamental component or noise. This paper has validated the practical application of the reference frame theory for diagnosing faults in electrical motors, demonstrating its precision in measuring both amplitude and phase. The experimental outcomes are compared with the results from a Fast Fourier Transform (FFT) spectrum analyzer to verify the method's accuracy. The is done for eccentricity and broken rotor bars faults.

Kim, Byunghwan, and colleagues, in their work [9], suggest an automated method to monitor the rotor condition of induction machines powered by a voltage source inverter when they are stationary. The proposed algorithm involves exciting the motor with pulsating fields at various angular positions to detect changes in the impedance pattern for identifying broken bars. But the method is being done under standstill condition and don’t seem efficient for online condition monitoring.

Motor Current Signature Analysis (MCSA) is becoming increasingly popular these days due to the simplicity of its variants, which typically only need a clamp meter for stator current detection. Moreover, the majority of diagnostic techniques based on MCSA are non-intrusive, allowing for online fault diagnostics without disrupting the ongoing process. Additionally, these methods incur lower computational costs [10].

For the examination of induction motors, machine learning-based defect diagnostic techniques were presented by Ali et al. [11]. In this work, two identical induction motors are subjected to a variety of single- and multi-electrical and/or mechanical failures in lab trials using the Discrete Wavelet Transform (DWT) for signal processing. During experiments, the motors' stator currents and vibration signals are measured simultaneously and used to build the fault diagnosis procedure. The data for unknown loading conditions that are not accessible in the experiment are found using a curve fitting equation. The study uses learning techniques from the MATLAB Classification Learner toolbox, such as SVM (support vector machine), K-nearest neighbors (KNN), and Ensemble classifiers, to assess the applicability and effectiveness of various classifiers in diagnosis of induction motor.

In [12] Asad, B. et al proposes the Improving Legibility of Motor Current Spectrum for Broken Rotor Bars Fault Diagnostics of induction machine. This study uses a band-stop filter in conjunction with the Fast Fourier Transform (FFT) to investigate the harmonic contribution of a broken rotor bar in an induction machine. Numerous harmonics are investigated, including winding, spatial, grid-fed, and fault-based harmonics. A logarithmic scale must be used since the fundamental component can obscure the spectrum because it is more potent than other frequencies. However, because of spectral leakage, there is a chance that this will obscure fault representative sideband frequencies. In order to alleviate this, the impact of the fundamental component is lessened by applying a band-stop Chebyshev filter, which improves the spectrum's clarity and comprehensibility even when seen on a linear scale. The filter effectively attenuates the main supply frequency with little effect on adjacent sideband frequencies thanks to its low passband ripples and good transition band. Simulations with a large number of mesh elements and very short step sizes are carried out using the finite element method to study the effect of the defect on magnetic flux distribution. Using the suggested method, the line current is calculated and the frequency spectrum is examined to distinguish between fault and spatial frequencies.

Chebyshev filters are recognized for their superior step response compared to Butterworth filters. The gain response of a Chebyshev filter as a function of frequency is expressed as follows:

$$G_n(\omega) = \frac{1}{\sqrt{1 + \varepsilon^2 T_n^2 \left(\frac{\omega}{\omega_0}\right)}} \tag{2.3}$$

where ε is ripple factor, ω_0 is cutoff frequency and Tn is its polynomial of n^{th} order.

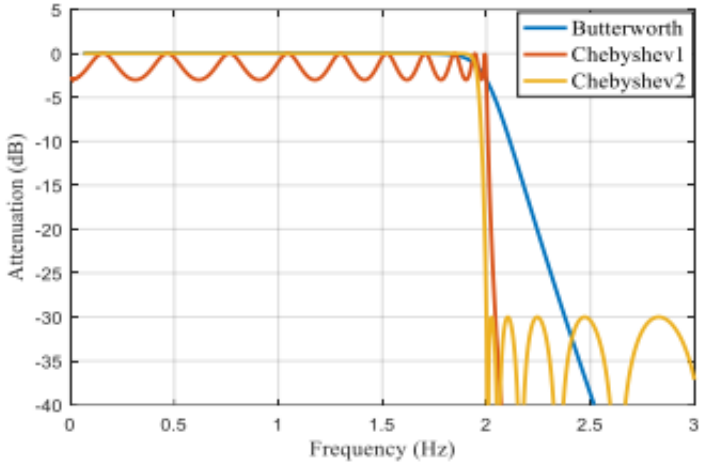

Figure 2.1 Step response comparison of the Butterworth and Chebyshev filters [12].

Figure 2.1 illustrates a comparison between Butterworth and Chebyshev Type I and Type II filters with identical tuning parameters. The Butterworth filter is evidently flat within its passband range but exhibits a less favorable roll-off, which can be problematic for fault frequencies situated very near the fundamental component, especially in cases of a broken rotor bar. On the other hand, the Chebyshev filters display an excellent transition band. However, they show ripples in both the pass band and stop band, present in both Type I and Type II variations. The reduced number of passband ripples in the case of the Type II filter lessens the influence of the filter on the frequency spectrum [12].

Bilal Asad et al in [5], study utilizes the optimal characteristics of the infinite impulse response (IIR) filter to effectively observe broken rotor bar (BRB) frequencies, ensuring clear legibility in the current and voltage spectra of both grid and inverter-fed motors. To gain a clearer insight, the origins of different harmonics in the stator current spectrum were analyzed. This analysis was grounded in both simulations and laboratory measurements. The findings revealed that by precisely adjusting IIR filters, diagnostic algorithms can be enhanced to identify specific frequencies. This is achieved by efficiently attenuating the fundamental component and minimizing its impact.

The study in [13] explores issues in induction machines, particularly those with broken rotor bars. The researchers used a mix of computer simulations, mathematical models, and real-world tests to understand the problems better. They developed a unique mathematical model that can predict the frequencies associated with broken bars, considering factors like the number of consecutive broken bars and speed variations.

The conclusion of the study introduces a new approach to identify the number of broken bars in a rotor. They found that certain components around the third current harmonic increase as more rotor bars break. Speed and torque also show changes with the number of broken bars. However, the authors highlight that high-frequency harmonics could be affected by skewing, a design feature in many rotors. They suggest further analysis to understand how skewing influences various harmonics, especially because skewed rotors are common in smaller machines. The researchers are currently working on this analysis and plan to share their findings soon. its spectral leakage.

Bilal A et al [4] have proposed a hybrid finite element method (FEM)–analytical model of a three phase squirrel cage induction motor solved using parallel processing for reducing the simulation time. The author has focused on the problem of AI based techniques requiring large no of data for the training of the algorithms. In order to validate the results, the frequency spectrum of the simulated stator current is compared with the one measured in the laboratory setup under healthy and broken rotor bar cases. To obtain these data, they used FEM simulation, and by splitting the rotor steps among several processors working in parallel, the simulation time reduces significantly.

The paper [14] by Asad et al. introduces an algorithm designed to enhance the frequency resolution of the spectrum for fault detection in electrical machines. This innovative approach aims to overcome challenges associated with low-power data acquisition devices, specifically utilizing smart sensors like Arduino cards, which are increasingly prevalent in the context of the Internet of Things (IoT), cloud computation, and Industry 4.0 standards.

The authors highlight the difficulty of detecting frequencies which represents the faults at the incipient stage due to their low amplitude and the leakage of energy from high frequency components into different bins of frequency. They propose an algorithm that addresses these issues without the need for complex signal processing techniques, making it suitable for device having low signal processing power. The paper presents result from both simulations and practical environments. The conclusion emphasizes the impact of low sampling frequency, fractional parts of the signal, and data discontinuities on spectral leakage when using the Fast Fourier Transform (FFT) algorithm. Spectral leakage, characterized by energy from one frequency leaking into nearby frequencies, can lead to inaccurate analysis and potential damage to electrical machines. The authors suggest applying a window function to mitigate these effects,

smoothing out abrupt changes at the edges of the analysis window. They acknowledge that some level of spectral leakage may persist even with a window function, depending on signal characteristics and the chosen window function. The paper concludes by showcasing how their simple algorithm effectively addresses these challenges and improves spectrum resolution.

The research [13] by Jaros et al focuses on monitoring the health of induction motors, a crucial aspect in the manufacturing industry to ensure efficient production. The authors explore various techniques and methods for condition monitoring, which involves assessing the performance and potential issues of these motors. This is particularly important for predictive maintenance (PM), a concept aimed at addressing problems before they lead to equipment failures. The article delves into the comparison of different approaches, considering measurements from both electrical and non-electrical sources. The goal is to process these measurements using advanced signal processing methods. The authors introduce their own testing setup, a controlled environment where they conduct experiments to gather data for analysis. They also outline their plans for creating datasets, emphasizing the importance of practical testing.

The article summarizes the findings and insights from the various techniques discussed. It highlights the advantages and disadvantages of different methods. The authors express their intention to apply these techniques to their own testbed, focusing on real-world measurements and sensor development. The research will involve using specific signal processing methods, like Wavelet Transform (WT), Empirical Mode Decomposition (EMD), Principal Component Analysis (PCA), and Park's Vector Approach (PVA), to handle the collected data effectively. Looking ahead, the authors emphasize the importance of classifying the signals and extracting crucial information about the induction motor's status. They plan to use different classifiers, including Support Vector Machines (SVM), Self-Organizing Maps (SOM), and Deep Neural Networks (DNN). These classifiers play a vital role in interpreting the signals and identifying potential issues with the motors. Overall, the article underscores the significance of advanced signal processing and classification techniques in ensuring the health and reliability of induction motors in manufacturing environments.

The literature on fault detection in induction motors (IM) has been a subject of extensive research over the past decades, driven by the critical role these electric machines play in industrial applications. Monitoring the condition of IM is essential for

diagnosing faults, and commonly employed techniques include vibration and stator current analysis. The subsequent signal processing aims to extract characteristic fault parameters, with the fast Fourier transform (FFT) serving as a prevalent method for spectrum analysis. However, the FFT comes with inherent limitations that have spurred continuous investigation into improving spectrum estimation methods.

One of the primary challenges associated with FFT-based analysis is its sensitivity to low signal-to-noise ratios, overlapping spectral components, non-stationary signals, and spectral leakage. While various studies have addressed these limitations to enhance spectrum estimation, the issue of spectral leakage has not received adequate attention, despite its potentially significant impact on the accuracy of fault detection. Spectral leakage occurs when the frequency of interest is not an exact multiple integer of the frequency resolution of the method, leading to undesired effects in the analysis.

In response to these challenges, the paper by Rene de J. Romero-Troncoso [15] introduces a novel methodology leveraging multirate signal processing techniques to enhance FFT-based spectral estimation for fault detection in induction motors. The proposed method involves multirate fractional resampling, achieved through a combination of interpolation and decimation applied to the stator current signal. The primary objective is to mitigate spectral leakage by adjusting the frequency resolution to align with the exact multiple integer of the frequency of interest. The experimental verification of the proposed approach shows its efficiency in enhancing FFT-based techniques for identifying faults in induction motors. By mitigating the problem of spectral leakage, the ability to detect fault-related spectral components is improved. This is especially important in situations where spectral components are closely spaced, such as with broken rotor bars. The experimental outcomes highlight the benefits of the proposed method, even in complex cases involving a combination of broken rotor bars and other mechanical issues like unbalance and misalignment, or when the motor is driven by an inverter.

The paper concludes by highlighting the broader applicability of the multirate fractional resampling methodology, suggesting its potential use in other applications such as power quality analysis. The proposed technique not only enhances spectral analysis but also effectively reduces spectral leakage, contributing to more accurate fault diagnosis in induction motors and potentially benefiting various signal processing applications beyond motor fault detection.

Raja, H.A.et al in [16] presents a signal spectrum-based machine learning approach to electrical machine fault prediction. The proposed method is a novel approach to electrical machine predictive maintenance. This paper describes the algorithm in detail and then validates its accuracy against data collected from operational electrical machines in both cases. A comparison of multiple machine learning algorithms used for training based on this approach is also provided at the end. They have described most challenging thing of real time monitoring of the electrical machine is the data collection. For the collection of the data the authors opened up a new research area known as the Internet of Things (IoT). These devices can not only communicate with each other, but they also can act as end nodes for data collection from electrical machines using sensors. In this paper they have generalized the maintenance of electrical machine into four phases as given in the Figure 2.2.

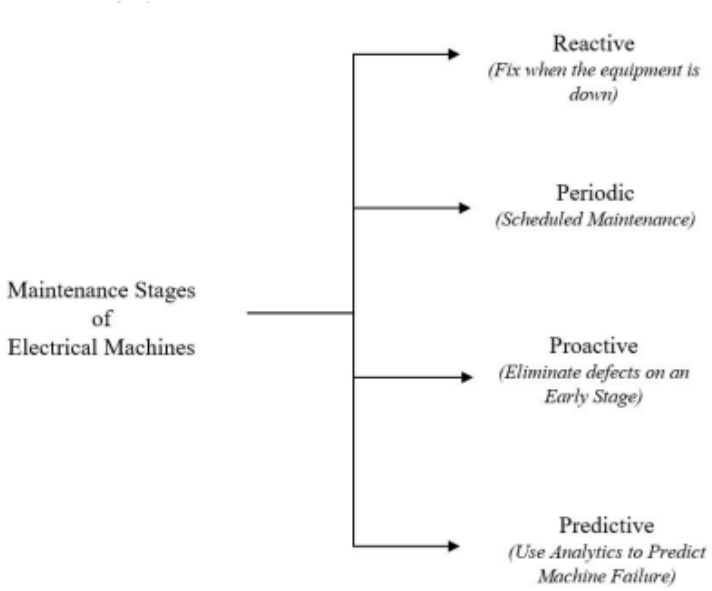

Figure 2.2: Maintenance phases of an electrical machine [16]

It is observed that every kind of faults introduces different harmonics and has a unique effect on the motor's overall signals, which include torque, speed, voltage, current, and speed. Even in the early phases of a fault, its presence can be determined by identifying certain frequency components. Table 2.1 lists the prevalent faults in induction machines and the their corresponding frequency modulations; further information on these faults can be found in [17] [18] [19].

Table 2.1: The fault signature frequencies for cage induction machines.

Type of fault	Fault Frequency component	Where
Broken rotor bars	$f_{BR} = f_s \pm 2ksf_s,$ $k = 1,2,3 \ldots\ldots$	k: Harmonic order f_s: Supply frequency f_{BR}: Broken bar frequencies f_{bbo}: Bearing outer race fault frequencies f_{bbi}: Bearing inner race fault frequencies f_r: Rotor frequency n_{bb}: Number of bearing balls s: slip p: Number of poles m: Positive integer
Eccentricity	$f_{ecce} = \left[1 \pm k\left(\frac{1-s}{p}\right)\right] f_s,$ $\frac{k}{p} = 1,3,5, \ldots\ldots$	
Bearing Faults	$f_{bbo} = f_s \pm 0.4kn_{bb}f_r,$ $k = 1,2,3 \ldots\ldots$ $f_{bbi} = f_s \pm 0.6kn_{bb}f_r \ , \ k = 1,2,3, \ldots\ldots$	
Inter- turn short circuit	$f_{st} = f_s \left[\frac{m}{p}(1-s) \pm k\right], k = 0,1,3,5 \ldots\ldots$	

2.1.1. Analysis of broken rotor bars fault

Induction motors are the backbone of industrial applications, widely used for their robustness, reliability, and efficiency. However, like any mechanical system, they are susceptible to various types of faults that can impact their performance and operational lifespan. One of the most common and detrimental faults in induction motors is the broken rotor bar (BRB) fault. This type of fault occurs when one or more of the bars in the rotor break or crack, leading to significant operational issues if not detected and addressed promptly.

Causes of Broken Rotor Bar Faults

Broken rotor bar faults can be attributed to several factors, including:

1. **Mechanical Stress**: The rotor bars are subjected to substantial mechanical forces during motor operation. Repeated starting and stopping cycles, particularly under high load conditions, can induce mechanical fatigue and lead to bar breakage.
2. **Thermal Stress**: High operating temperatures and poor cooling can cause thermal

expansion and contraction in the rotor bars, contributing to material fatigue and cracking over time.

3. **Manufacturing Defects**: Imperfections during the manufacturing process, such as poor casting or welding defects, can result in weak spots in the rotor bars that are prone to breaking under operational stress.
4. **Electrical Stress**: Electrical imbalances and transient overcurrent can create excessive electromagnetic forces, which can weaken and eventually break the rotor bars.

Consequences of Broken Rotor Bar Faults

The presence of broken rotor bars can have several adverse effects on the motor's performance, including:

1. **Reduced Efficiency**: Broken rotor bars disrupt the uniform distribution of currents in the rotor, leading to increased losses and reduced motor efficiency.
2. **Vibration and Noise**: The imbalance caused by broken rotor bars often results in increased vibration and noise levels, which can further damage the motor and connected machinery.
3. **Overheating**: The uneven current distribution can cause localized overheating in the rotor, exacerbating the fault and potentially leading to catastrophic motor failure.
4. **Performance Degradation**: Broken rotor bars can lead to torque pulsations and reduced torque output, affecting the motor's ability to drive loads effectively.

In this research the study of broken rotor bars faults is performed. Depending on the defect's severity, each failure causes a different frequency and modulation index in the stator current. The geometric and electrical parameters of the rotor and stator determine the mathematical representation of these fault frequencies. Early detection of a broken bar is crucial because when one breaks, the subsequent bars are subjected to increased thermal stress, which may lead to their failure. Certain harmonics in the frequency spectrum are produced by these faults [20].

$$f_{br} = f_s \pm 2ksf_s \tag{2.1}$$

$$f_{br} = \left[\left(\frac{k}{p}\right)(1-s) \pm s\right] f_s \tag{2.2}$$

where p is the number of pole pairs in the machine, s is the slip, and fs is the supply frequency for k = 1, 2, 3,... The broken rotor bar causes the lower sideband to appear, and the ensuing speed fluctuations cause the upper sideband to appear. The left side band (LSB) and right side band (RSB) are the fault-related harmonics. These fault harmonics can be buried under fundamental frequency spectrum because of their dependency on slip. These problem is more severe for the motor running under the low load condition.

In [12] the author performs the FEM simulation of motor that utilizes 2D field analysis, with the effects of the neglected end windings accounted for by incorporating extra resistances and inductances in series with the coils. The stator coils, configured per phase, consist of copper strands connected in series and parallel, ensuring a uniform distribution of current density. This simulation is conducted at a constant speed under rated load conditions. Figure 3 illustrates the flux distribution for both healthy and two broken rotor bar scenarios. The results indicate a rise in flux density around the broken bars, which subjects the adjacent bars to increased magnetic stress. This stress elevation leads to higher currents in the neighboring bars, posing a risk of further bar breakage over time if the fault is not detected and repaired promptly.

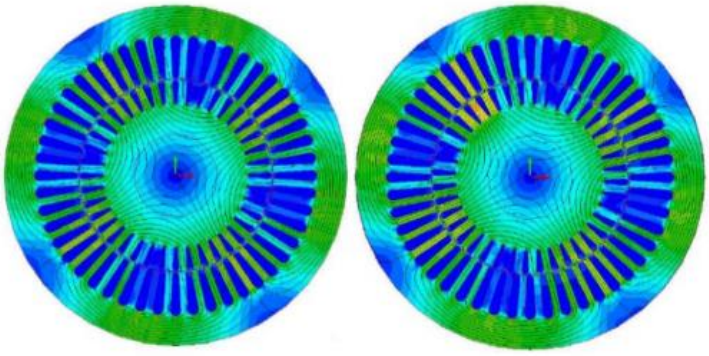

Figure 2.3 . Normalized magnetic field density in healthy and motor with broken rotor bar [12].

Some of the literature based on condition monitoring approach using motor current signature analysis (MCSA) for the detection of broken rotor bars fault in induction motor is presented here. The paper [21] discusses the limitations of traditional steady-state fault detection techniques and emphasizes the advantages of analyzing the start-up transient current, which can reveal faults not detectable during steady-state conditions. Utilizing Finite Element Method (FEM) modeling with Maxwell2D software, the paper underscores the importance of accurate modeling, which is further

enhanced by optimizing broken rotor bar parameters using Genetic Algorithms (GA). This approach ensures the model closely mirrors real-world motor conditions. Additionally, the paper highlights the application of Discrete Wavelet Transform (DWT) for analyzing stator current signals, facilitating the identification of specific frequency signatures associated with rotor bar failures. By decomposing the stator current signal, DWT provides detailed insights necessary for early fault detection. The integration of these techniques within simulation environments such as MATLAB/SIMULINK allows for comprehensive validation and refinement of the proposed fault detection methods. Consequently, the study demonstrates that the combined use of FEM, GA, and DWT enables accurate and immediate detection of rotor bar failures during both steady-state and transient conditions, significantly enhancing motor system reliability and reducing maintenance costs.

The paper [22] explores the effectiveness of Motor Current Signature Analysis (MCSA) combined with Fast Fourier Transform (FFT) in diagnosing BRB faults. Induction motors are integral in various applications due to their robustness and adjustable speed drives, making early fault detection crucial to prevent economic and safety issues. The study highlights the application of FFT to various signals such as current, power, vibration, and electromagnetic torque to identify BRB faults. By focusing on the frequency-domain analysis, particularly the components harmonics influenced by slip value, the research offers new insights into the spectral content of the stator current under fault conditions. In their experimental setup, the authors analyzed the induction motor's performance under different states (no load, load, healthy, and defective) to validate their approach. The conclusion drawn from the study indicates that spectral analysis using FFT can effectively detect characteristic harmonics in the stator current spectrum, which are indicative of BRB faults. The presence of sideband frequencies around the fundamental frequency and their relation to slip values were key in diagnosing the severity and presence of faults. The study confirms that these characteristic frequencies are highly dependent on the motor's operating conditions, emphasizing the importance of analyzing both stationary and non-stationary regimes. This comprehensive approach ensures accurate early detection of BRB faults, thereby enhancing motor reliability and performance.

2.2. Vibration Analysis

Vibration analysis offers valuable insights into the condition of electrical equipment

and is therefore extensively utilized for diagnostics. In an electrical machine, vibrations can originate from various sources, including magnetic fields, fluid flow, imbalances, and particularly rotating components like bearings, gearboxes, or rotors [23]. Vibration analysis involves monitoring changes from established vibration signatures and identifying deviations within the system. These deviations are detected in terms of acceleration amplitude, frequency value, and intensity. This paper by Martinez. et al [24] introduces a formula that connects the vibrations in the stator of an induction machine to the number of broken bars in its rotor. The formula considers both the amplitudes and frequencies of vibrations, and its accuracy is confirmed through numerical simulations and real-world experiments. The study reveals that the vibration amplitudes of certain frequency components increase quadratically with the number of broken bars, especially under rated load conditions. The targeted frequency components range from two to four times the supply frequency, making the implementation feasible with affordable instrumentation. The paper's key contributions lie in deriving these analytical equations, validating them through numerical analysis, and comparing the results with actual experimental measurements.

2.3. Fast Fourier Transform

In numerous scientific fields, the Fast Fourier Transform (FFT), is a useful tool. It assists in splitting an erratic signal into distinct components known as sinusoids. Amplitude is the term used to describe the frequency and size of these sinusoids. These sinusoids typically get smaller in size as we examine across a range of frequencies. The foundational component is the most significant. This process is represented mathematically by formulas known as the discrete Fourier transform (DFT) and its inverse.

$$\mathrm{X_k} = \sum_{n=0}^{N-1} x_n \, e^{-\frac{j2\pi kn}{N}}, \mathrm{k} = 0, 1, 2, \ldots\ldots\ldots (\mathrm{N}-1), \tag{2.4}$$

$$\mathrm{x_n} = \frac{1}{N}\sum_{n=0}^{N-1} X_n \, e^{-\frac{j2\pi kn}{N}}, \mathrm{k} = 0, 1, 2, \ldots\ldots\ldots (\mathrm{N}-1), \tag{2.5}$$

where k is the current frequency, N is the number of samples, n is the current sample, x_n is the signal value at time n, and X_k is the DFT resulting bin, for a comprehensive and precise frequency spectrum, frequency resolution is crucial. It is determined by the measurement duration of the signal and the sampling frequency, as illustrated by the following equation.:

$$\Delta f = \frac{1}{T_m} = \frac{f_s}{N} \tag{2.6}$$

Where Δf represents the difference of two consecutive frequency bins, N is the no of samples and fs is the sampling frequency. As the signal under consideration has a limited duration, and this duration may not evenly fit multiple cycles of all frequency components, a challenge known as spectral leakage arises. The fundamental component, being the most prominent, is particularly prone to experiencing greater spectral leakage.

CHAPTER THREE: METHODOLOGY

The overall research methodology followed during the research is as following:

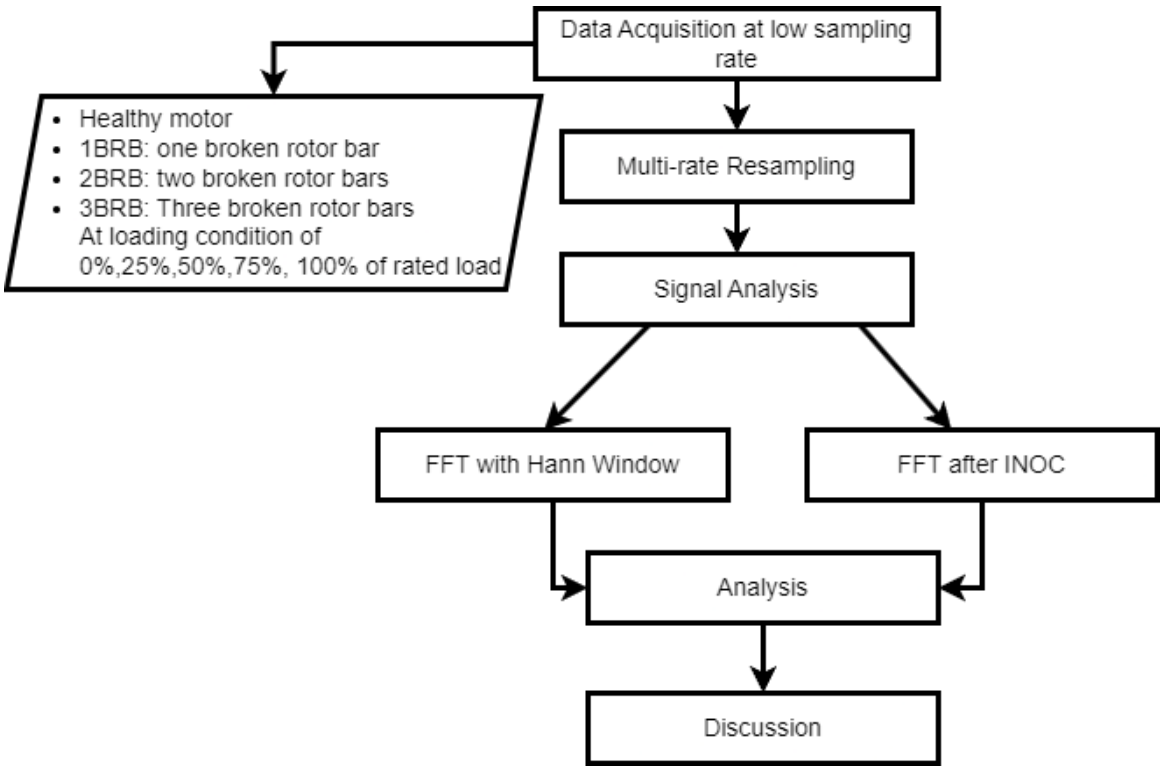

Figure 3.1: Flowchart of Methodology

3.1. Data Acquisition

The data for the research is provided by the Department of Electrical Engineering and Automation, Aalto University, Finland under the project Capacity Enhancement of Electrical Equipment Condition Monitoring and Fault Diagnostics (CEEECoM). The data were taken at laboratory of Tallinn University, Tallinn, Estonia. Each test setup includes two identical motors, and you can find details about their specifications in Table below. In this setup, one motor is being studied, while the other is used as a load. Both motors are placed on the same mechanical base and connected through their shafts, as shown in

Figure 3.3 and Figure 3.2. To enhance control over the load, the loading motor is powered by inverters. The machine under investigation is powered by grid and

industrial inverters, each operating under different control mechanisms. The Dewetron transient recorder is used to measure the stator currents and voltages.

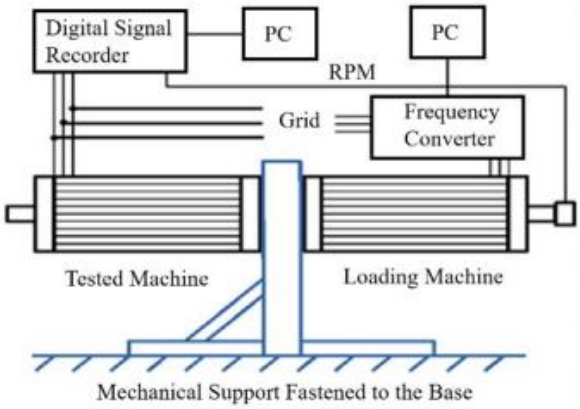

(a)

(b)

Figure 3.2: (a) Block diagram of the setup, (b) The experimental setup

(a) (b)

Figure 3.3: (a) The rotor with two broken bars, (b) The rotor with three broken bars

Table 3.1: Specification of the motor

Parameters	Symbol	Value
No of poles	P	4
Number of Phases	ψ	3
Connection	Y -Δ	Delta
Voltage	V	400
Frequency	Hz	50
Current	A	15.3
Power	KW	7.5
Speed	rpm	1460
Power factor	cosφ	0.79

The broken rotor bars are created by drilling the rotor of the motor as shown in Figure 3.3: (a) The rotor with two broken bars, (b) The rotor with three broken bars The sampling rate of the measured signal is 20000 per seconds (20KHz) and measurement time is about 20 seconds. The stator currents for the following different cases are measured.

- Healthy
- 1BRB: Motor with one broken rotor bar
- 2BRB: Motor with two broken rotor bars
- 3BRB: Motor with three broken rotor bars

The data is collected for loading condition of 0%, 25%, 50%, 75%, and 100% of the rated load for each of the cases mentioned above.

For my study first step is to down sample the acquired data at the sampling rate of 20 kHz to the sampling rate of 2 KHz. It is to make the acquired data are measured at the low sampling rate and improve the sample rate later as required. To address the problem associate with low sampling rate resampling is done based on the literature [15]. The process to change the sample rate is called resampling which is performed using multi-rate resampling.

3.2. Multi-rate resampling

The concept of the multi- rate resampling for signal processing is provided by Rene de J. Romero-Troncoso in [15]. The resampling is done by using the combination of decimation and interpolation as below.

$$f_r = \frac{q}{p} f_s \tag{3.1}$$

Where fr is the resampled frequency, p is the integer interpolation factor, q is the integer decimation factor and fs is the sampling frequency. Hence by using decimation and interpolation a fractional resampling can be performed to get the desired sampling frequency.

3.2.1. Decimation

The inverse multi-rate signal processing method to the interpolation is known as decimation. In this technique, the number of original samples is reduced by an integer factor, denoted as 'p.' Decimation involves either selecting one sample and discarding the other p-1 which is also called down dawn sampling of the samples or averaging the p samples which can be done by using decimate function in MATLAB. The latter is preferred as it helps diminish quantization noise [15]. Decimation also have following advantages over the down sampling.

- Decimate combines low-pass filtering and downsampling in a single step, enhancing efficiency.
- Decimate offers a straightforward approach to downsampling, minimizing the need for complex interpolation methods.
- Attenuates higher-frequency components, preventing aliasing effects and maintaining signal integrity.

When decimating p times, the sampling frequency decreases to fr = fs / p, thereby reducing the original signal's bandwidth by a factor of p. The example of decimation of 20 KHz data by the factor of 10 is shown in Figure 3.4.

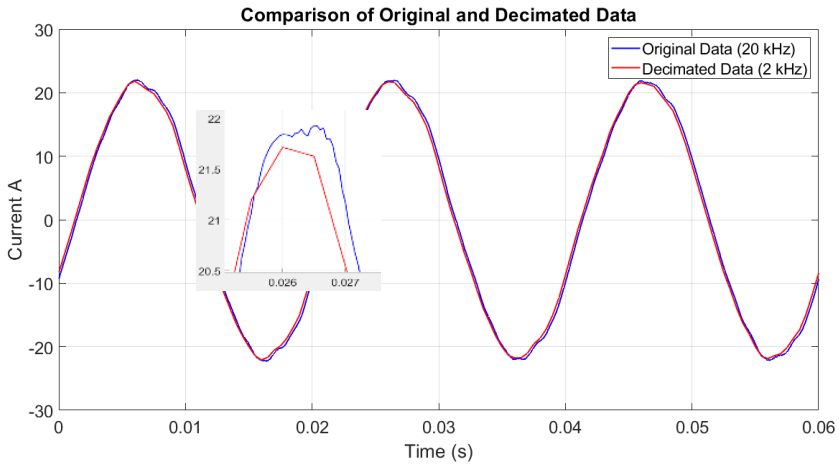

Figure 3.4: Comparison of original and decimated data

3.2.2. Interpolation

In signal processing, interpolation is a method used to estimate or create values between sampled points in a signal, which helps in the signal's reconstruction or enhancement. An interpolation with a rate of q involves a multirate signal process that generates samples between two original samples. [15]. Therefore, interpolating of q times, the signal frequency fs is resampled fr as:

$$f_r = qf_s \tag{3.2}$$

There are various types of interpolation techniques among the main interpolation techniques that are compared in this study are linear interpolation, cubic interpolation and spline interpolation.

1. Linear Interpolation

Linear interpolation connects two adjacent data points with a straight line. Given two data points (x_0, y_0) and (x_1, y_1), the linearly interpolated value (y) at a point x between x_0 and x_1 is given by:

$$\boldsymbol{y} = \mathrm{y}_0 + (\mathrm{x} - \mathrm{x}_0)\frac{\mathrm{y}_1 - \mathrm{y}_0}{\mathrm{x}_1 - \mathrm{x}_0} \tag{3.3}$$

2. Cubic Interpolation

Cubic interpolation uses a cubic polynomial to interpolate between adjacent data points. Given four data points (x_0, y_0), (x_1, y_1), (x_2, y_2), and (x_3, y_3), the cubic interpolated value (y) at a point x between x_1 and x_2 is given by:

$$y = a_0 + a_1(x - x_1)^1 + a_2(x - x_1)^2 + a_3(x - x_1)^3 \tag{3.4}$$

*a*0, a1, a2, a3 are coefficients determined based on the surrounding data points.

3. Spline Interpolation

Spline interpolation uses piecewise-defined polynomial functions, typically cubic polynomials, to interpolate between data points. A common method is the cubic spline interpolation. The interpolated value y at a point x within the segment $[x_i\ , x_{i+1}]$ is given by:

$$S(x) = a_i + b_i(x - x_i) + c_i(x - x_i)^2 + d_i(x - x_i)^3 \tag{3.5}$$

Where a_i, b_i, c_i, d_i are coefficients determined by solving a system of equations based on the values at the adjacent data points.

Figure 3.5 gives the comparison between the different interpolation techniques. From this we can say that for the sinusoidal signal cubic and spline interpolation are the better choice for the interpolation techniques but the calculation burden for cubic and spline will be more than that of linear interpolation.

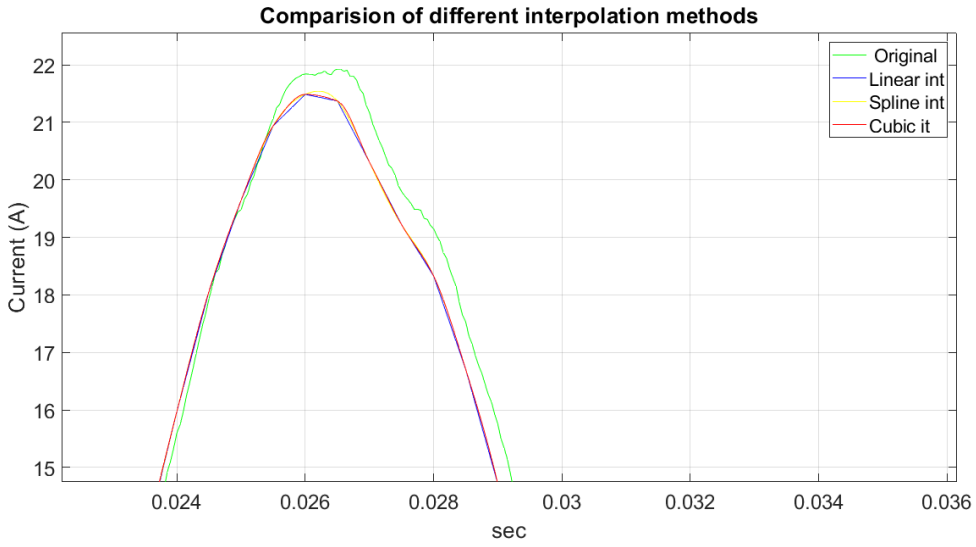

Figure 3.5: Plot of different interpolation techniques

Figure 3.6 gives the improvement in the smoothness of the signal after interpolation of low sampling rate data.

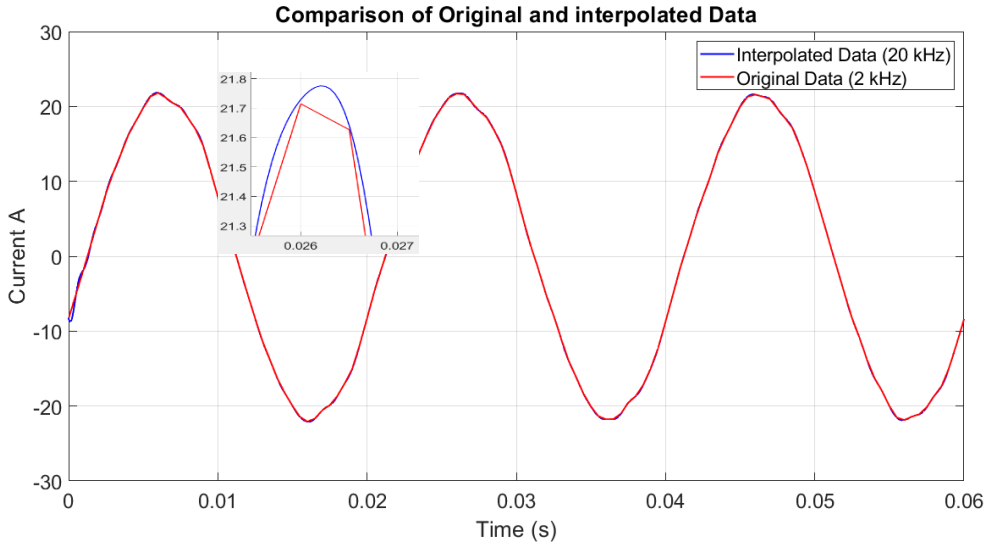

Figure 3.6: The plot of current data before and after data interpolation

The interpolation technique does not only improve the smoothness of the signal but also refine the zero crossing as shown in the Figure 3.7.

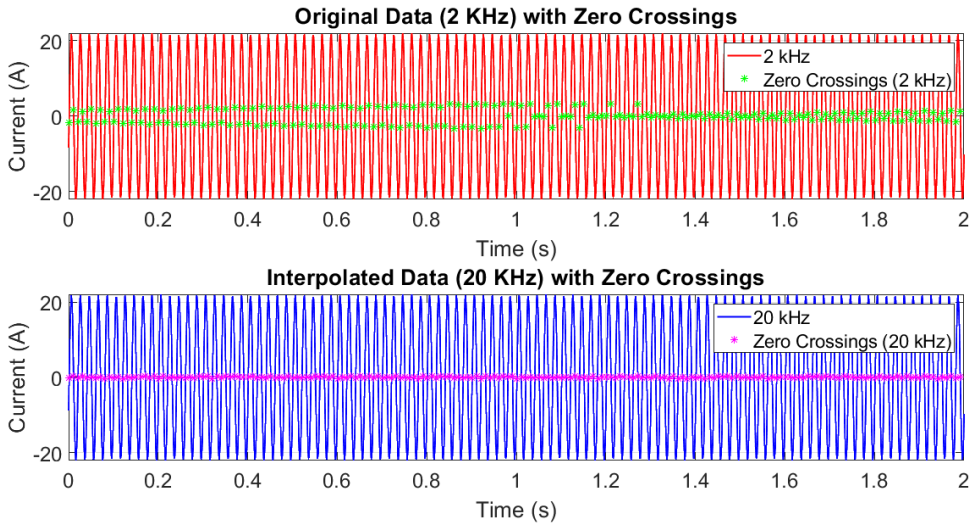

Figure 3.7: Current and approximate zero crossing at a sampling frequency of 2 KHz and 20 KHz

3.2.3. Fractional resampling

Interpolation and decimation can be combined to obtain the multi-rate resampling. After interpolation of the low sampling rate, the fractional resampling can be performed which will help in reducing the spectral leakage. The spectral leakage becomes null only in those cases when the characteristic frequency component (f_x) is an exact multiple integer (M) of the frequency resolution of FFT, which depends on the window length of the FFT and frequency of sampling f_s [15]as given below:

$$f_x = M\frac{f_s}{N} \tag{3.6}$$

Here when the value of M becomes exact integer, the spectral leakages will be negligible [29]. Such that using fractional resampling we will get the resulting frequency Δf_r as:

$$\Delta f_r = \frac{f_s}{N}\frac{q}{p} \tag{3.7}$$

$$f_x = M\,\Delta f_r \qquad s(3.8)$$

Hence by choosing the proper value of p and q, we can make the value of M exact integer before performing the FFT using windowing techniques. Here one of the things to consider for interpolation is Interpolating a signal may lead to spectral distortion as a result of inherent mathematical principles and limitations in the interpolation process. Factors such as signal aliasing or temporal variations in the signal can contribute to this

distortion. Consequently, the interpolation process may introduce quantization noise into the signal [15]. To mitigate the effects of interpolation and minimize spectral distortion, it becomes crucial to incorporate a Low-Pass Filter (LPF). The LPF, with a specified cut-off frequency plays a significant role in addressing these interpolation effects. Hence for the process of interpolation resample function is used in this research as it contains the FIR Antialiasing Low Pass Filter.

3.3. Signal Analysis

Signal analysis of electrical signals involves studying and processing electrical waveforms to extract meaningful information. Various types of signal processing techniques like Fast Fourier Transform (FFT), Wavelet Transform (WT), Park's Vector Approach (PVA) can be found to study the broken rotor bars fault in the literature. For our study FFT is used as signal analysis techniques in this research.

Why FFT?

The Fast Fourier Transform (FFT) is a cornerstone in signal processing due to its efficiency and effectiveness in converting time-domain signals into their frequency-domain representation. Here's why FFT is particularly suitable for our signal analysis:

1. **Frequency Domain Analysis**: Motor current signals often contain information about the motor's condition encoded in specific frequency components. FFT allows us to identify and analyze these components, such as fundamental frequencies and harmonics, which are crucial for detecting faults.
2. **Efficiency**: FFT is computationally efficient, capable of handling large datasets quickly. This efficiency is essential when processing high-resolution motor current signals, particularly in real-time monitoring and diagnostics applications.
3. **Harmonic Detection**: Faults in electric motors, such as broken rotor bars, generate characteristic harmonics in the current signal. FFT is adept at isolating these harmonics, enabling precise fault detection and diagnosis.
4. **Spectral Leakage Reduction**: By using window functions and techniques like resampling, FFT can be tailored to reduce spectral leakage, improving the accuracy of frequency component identification.

Given these advantages, FFT serves as the backbone of our signal analysis approach, providing a robust and reliable method for transforming and interpreting motor current

signals.

The frequencies in the signal and how often we measure or sample that signal need to match up properly. Getting perfect matching data is hard because of limits in our measuring tools and some unwanted signals called noise. To fix this mismatch, we can use something called windowing techniques. But it's not as simple as it sounds; choosing the right window is crucial to make sure we get a clear picture of the main signal without extra unwanted signals. Dealing with these issues requires special knowledge about how windowing works and how it affects the signal picture. Unfortunately, there's no one-size-fits-all solution. One problem with a technique called FFT is that if the sampling frequency and signal frequency don't match well, it can lead to some blurriness in the signal picture, which we call spectral leakage [14]. Considering the low sampling rate of the signal following method is also proposed for FFT analysis to improve the spectrum of the signal which is compared with FFT with Hann Window after multi-rate resampling and FFT with proposed technique.

3.3.1.FFT after counting integral number of cycle

This is the proposed techniques highlighting the objectives of this research. In signal processing, accurate frequency domain analysis is critical for diagnosing and analyzing electrical signals, particularly in the context of motor diagnostics. One of the primary techniques used for this purpose is the Fast Fourier Transform (FFT), which converts a time-domain signal into its frequency-domain representation. However, the accuracy and resolution of FFT can be significantly affected by spectral leakage, a phenomenon where energy from one frequency bin spills into adjacent bins, leading to a distortion of the spectral information.

Spectral leakage is particularly problematic when the signal length does not correspond to an integral number of cycles of the underlying periodic components. This discrepancy introduces discontinuities at the boundaries of the signal segment, exacerbating leakage and degrading the quality of the frequency spectrum. To address this issue, the methodology of counting Integral Number of Cycles (INOC) is employed.

The INOC approach ensures that the signal segment analyzed by FFT contains an integer number of cycles of the fundamental frequency. By carefully selecting the segment's start and end points based on zero crossings, we can minimize discontinuities

and thus reduce spectral leakage. This method involves the following steps:

1) Initially, we compute the integral cycles and the signal's length, ensuring suitable prime factors. The signal's fractional components at the beginning and end lead to a decline in the resolution of the spectrum. Additionally, an unsuitable signal length with numerous or large prime factors hampers the efficiency of FFT (Fast Fourier Transform), escalating complexity, memory demands, and calculation duration.
2) A low sampling frequency can lead to poor frequency resolution and more spectral leakage. This is mainly due to sharp changes in the acquired signal. To address this issue, it is proposed to eliminate these sharp changes using data interpolation. By employing data interpolation, we can simulate only the necessary steps and approximate the remaining values. As we have discussed already data interpolation also refine the zero crossing point.
3) The presence of fractional parts at the beginning or end of the signal amplifies spectral leakage and intensifies the need for a windowing function. The number of cycles can be calculated as:

$$J = M\frac{f_{int}}{f_s} = J_{int} + \Delta$$

Where, J represents the total number of cycles, fin is the frequency of the fundamental component in a nearby sinusoidal signal, fs is the sampling frequency, M denotes the length of the recorded signal, Jint signifies the integral number of signal cycles, and Δ represents the fractional part. The presence of a non-zero Δ contributes to spectral leakage. The first purpose is to discard the fractional part Δ by calculating Jint in the acquired signal.

To discard the starting and ending fractional cycle first step is to find the zero crossing of the signal and save the signal from the first zero crossing to last zero crossing eliminating the remaining parts.

4) For integral no of cycle first count the no of zero crossing nz then If nz is even, save the signal till the second last zero crossing. We can see the plot of the figure after counting the integral no of cycle and removing starting and end fractional cycle in Figure 3.8.

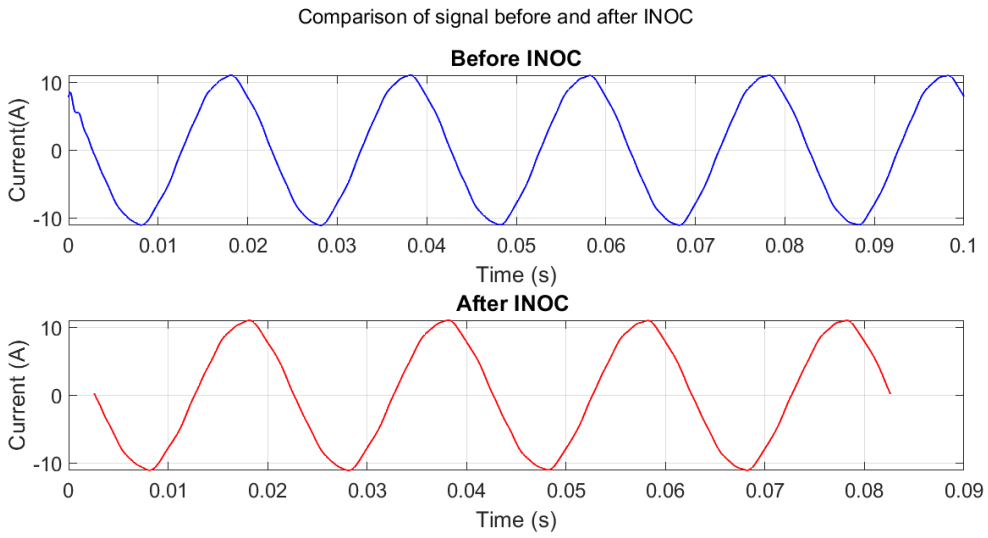

Figure 3.8: Plot of signal after counting the integral no of cycle

The main proposed algorithm of this research is shown in Figure 3.9. Its primary components include the eliminatin of the DC offset, which decreases the likelihood of having a frequency bin at 0 Hz in the spectrum, removal of starting and ending fractional parts which increase the spectral leakage.

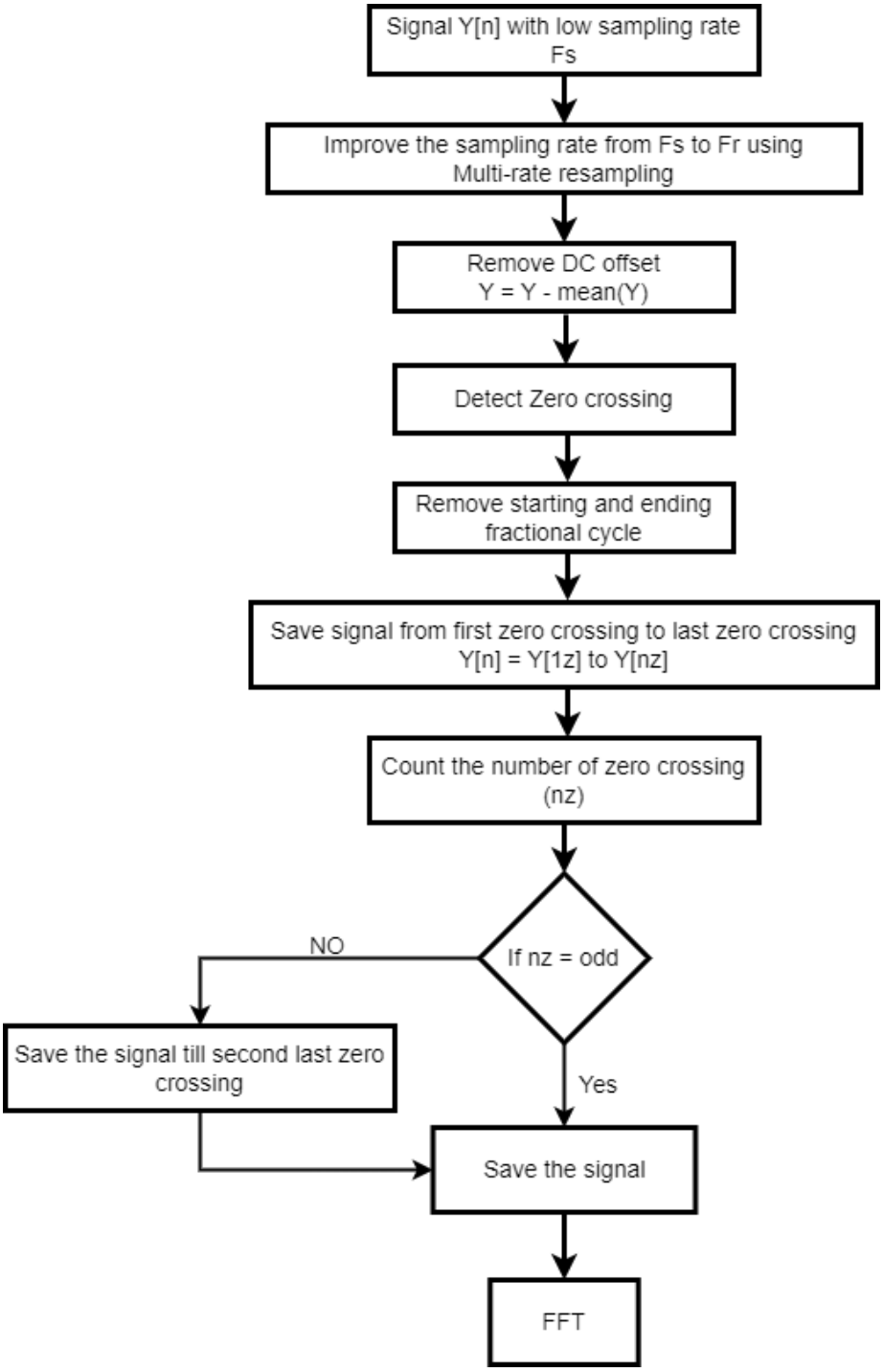

Figure 3.9: Flowchart for improvement of the spectral resolution

3.3.2. FFT with Hann window after multirate resampling

This technique serves as the benchmark for the comparison. In this method the FFT of the data obtained is plotted with the use of Hann Window function after multirate resampling. The Hann window is a type of tapering function used to smooth discontinuities at the boundaries of the signal, minimizing spectral leakage and enhancing the clarity of the frequency spectrum. By applying the Hann window before performing FFT analysis, we further improve the accuracy and reliability of frequency analysis. The Hann window's ability to attenuate side lobes and sharpen the main lobe of the spectrum makes it an invaluable tool for enhancing the interpretability of FFT results. The frequency spectrum obtained after the use of multirate resampling are sharper and the fault harmonics are more visible then with only use the Hann function without use of multirate rate resampling [15].

Hann Window

In signal processing, window functions play a critical role in the analysis of finite-length signals. One of the most commonly used window functions is the Hann window, also known as the Hanning window. Named after Julius von Hann, the Hann window is a type of tapering function that helps to mitigate the issues associated with spectral leakage in the Fourier Transform.

Spectral leakage occurs when the discrete Fourier Transform (DFT) assumes that the finite signal is periodic, which often leads to discontinuities at the boundaries of the signal segment. These discontinuities introduce artificial high-frequency components, distorting the frequency spectrum. The Hann window addresses this problem by applying a smooth taper to the signal's edges, thereby reducing the abrupt transitions at the boundaries.

Mathematically, the Hann window w[n] is defined as:

$$\mathrm{w[n]} = 0.5\left(1 - \cos\left(\frac{2\pi \mathrm{n}}{N-1}\right)\right)$$

Where n ranges from 0 to N-1. N is the total number of samples. This equation ensures that the window smoothly tapers the signal to zero at the beginning and end of the segment.

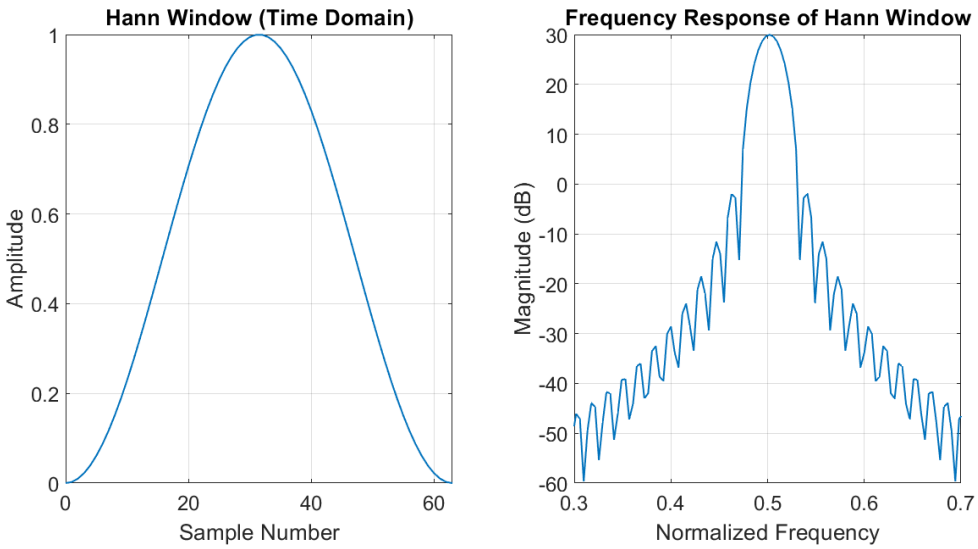

Figure 3.10: Plot of a sample of Hann Window in time domain and frequency domain

The primary advantage of the Hann window is its ability to minimize the side lobes in the frequency domain, which are the primary source of spectral leakage. By reducing these side lobes, the Hann window enhances the resolution of the main lobe, making it easier to distinguish between closely spaced frequency components. This property is particularly useful in applications such as motor diagnostics, where accurate identification of fault harmonics is crucial.

In summary, the Hann window is an effective tool for improving the accuracy of frequency analysis in FFT applications. By applying this window function, we can achieve clearer and more reliable spectral representations, facilitating better diagnosis and analysis of signals in various engineering and scientific fields.

Figure 3.11 illustrates the comparison of the signal spectrum with and without the application of the Hann window for a motor with one broken rotor bar (1BRB) under different loading conditions: 100%, 50%, and 25%.

The application of the Hann window significantly enhances the quality of the spectrum. Without the Hann window, the spectra exhibit considerable spectral leakage, making it challenging to distinguish the fault harmonics, especially at lower load conditions. Spectral leakage manifests as broadening and smearing of spectral lines, which can hamper the critical diagnostic information. Here, the spectra obtained with the Hann window demonstrate a certain reduction in spectral leakage. The tapering effect of the Hann

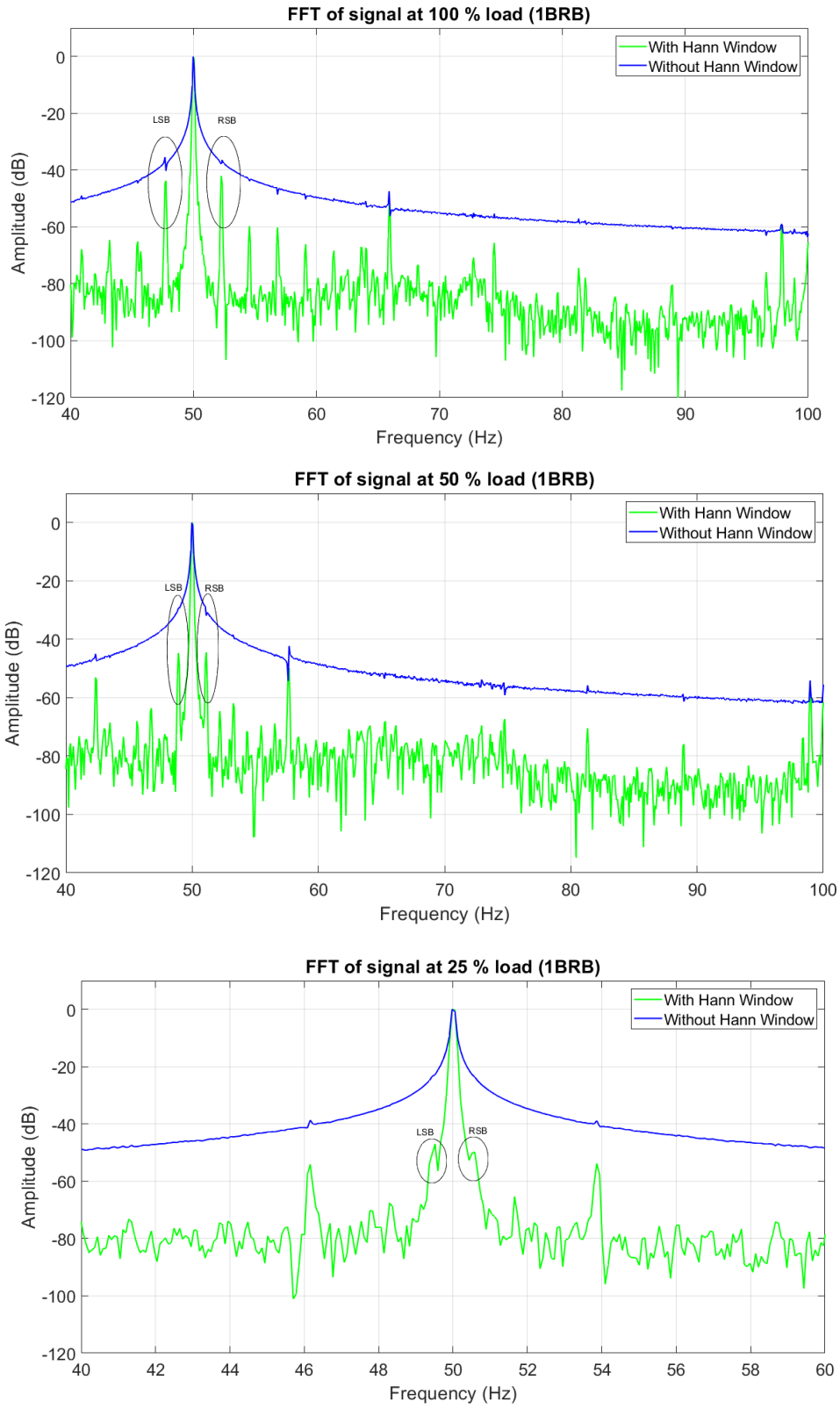

Figure 3.11: Comparison of signal spectrum with and without Hann Window for different loading condition of motor with 1BRB

window smooths the transitions at the boundaries of the signal segment, thereby

minimizing the introduction of artificial high-frequency components. This results in sharper and more distinct spectral lines.

As a consequence, the bands corresponding to fault harmonics become more clearly visible across all loading conditions. This improvement is particularly pronounced at the lower load conditions (50% and 25%), where fault harmonics are typically less visible due to lower signal amplitude and higher relative noise. Additionally, at low load conditions, the slip is low, which causes the side fault bands to be closer to the fundamental frequency. This proximity makes the sidebands less visible without the Hann window due to their overlap with the fundamental component. The Hann window's ability to reduce spectral leakage and enhance resolution ensures that these sidebands remain distinguishable even when they are close to the fundamental frequency.

Overall, Figure 3.11 demonstrates that the use of the Hann window significantly improves the spectral quality, making it a valuable tool in signal processing for motor diagnostics. The clear visibility of fault bands, even under low load conditions, underscores the effectiveness of the Hann window in maintaining diagnostic clarity.

In this method the FFT of the current data is obtained in such a way that the fundamental frequency will be exact integer multiple of the frequency resolution and the window length will be exact power of two. To make this happen the sampling frequency is resampled in following way.

We know from (3.7) and (3.8),

$$f_r = f_s \frac{q}{p}$$

$$\Delta f_r = \frac{f_s}{N} \frac{q}{p}$$

$$f_x = M * \Delta f_r$$

Where f_s is sampling frequency, f_r is resampled frequency, Δf_r is frequency resolution after resampling, q and p are the interpolation and decimation factors and fx is the fundamental frequency. For our case,

fs = 20000 Hz

N = exact power of two

fx = 50 Hz

Table 3.2: Frequency Resolution for different sampling rate

Sampling Frequency fs (Hz)	Window Length(N)	Frequency Resolution (Hz)	M
20000	32768	0.6104	81.9135
	65536	0.3052	163.827
	131072	0.1526	327.654
16384	32768	0.5	100
	65536	0.25	200
	131072	0.125	400

Now the nearest frequency resolution near to 0.6104 that makes M the exact integer is 0.5 and similarly for N = 65536, 131072, 131072 the frequency resolution obtained will be 0.25, 0.125 and 0.0625 respectively. For this the resampled frequency must be 16384 Hz. This can be obtained by q = 512 and p = 625. The whole calculation is shown in Table 3.2

Advantages for Comparison:

- **Improved Frequency Resolution:** The combination of multirate resampling and the Hann window enhances frequency resolution, allowing for more accurate identification of fault-related harmonics and other frequency components. This improvement in resolution makes it easier to compare results obtained from this methodology with those from our main methodology in section 3.3.1.
- **Reduced Spectral Leakage:** Multirate resampling and the Hann window minimize spectral leakage, resulting in clearer and more distinguishable frequency spectra. This reduction in leakage facilitates a more precise comparison between the two methodologies, enabling us to evaluate their respective effectiveness in fault diagnosis and signal analysis.
- **Enhanced Interpretability:** By improving frequency resolution and reducing spectral leakage, this approach enhances the interpretability of FFT results, making it easier to identify and analyze frequency components. This enhanced interpretability facilitates a more insightful comparison between the methodologies, allowing us to draw meaningful conclusions regarding their relative performance.

Given its advantages in frequency resolution, spectral leakage reduction, and interpretability, the FFT with Hann Window after Multirate Resampling approach serves as a suitable benchmark for comparison with our primary methodology FFT after counting integral number of cycle The results showing the improvement after the mutirate resampling is discussed later in the results and discussion. By comparing the results obtained from these two methodologies, we can gain valuable insights into their relative effectiveness in electric motor diagnostics and fault analysis

CHAPTER FOUR: RESULTS AND DISCUSSION

In this research the signal analysis using FFT by three different approaches are studied for different cases which are:

- Simple FFT.
- FFT with Hann Window after multi-rate resampling.
- FFT after proposed algorithm.

Here cases of the study are:

1. 0BRB: Healthy motor
2. 1BRB: Motor with one broken rotor bar
3. 2BRB: Motor with two broken rotor bar
4. 3BRB: Motor with three broken rotor bar

At loading condition of 0%, 25%, 50%, 75%, and 100% of rated load for each cases.

4.1. Case 1: Healthy motor

First the proposed method is studied using the data obtain from healthy motor for different loading condition.

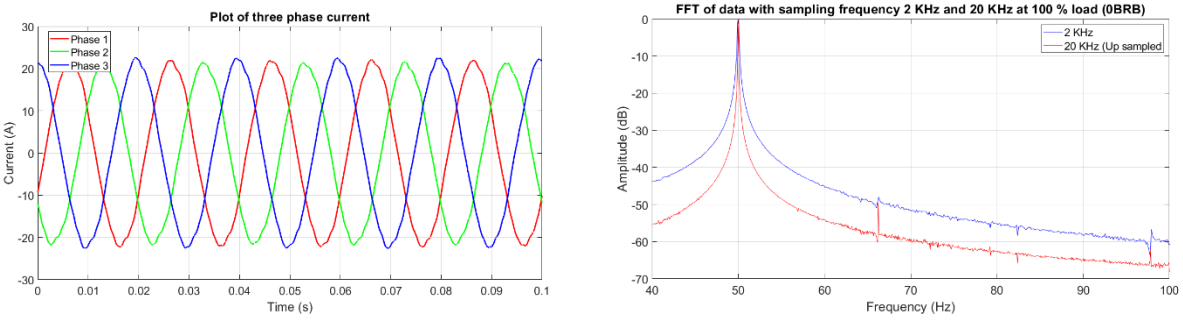

(a) (b)

Figure 4.1: (a) 3 phase current plot of healthy motor at 100 % load, (b) FFT plot of current signal at 2KHz and 20 KHz (Up sampled)

Figure 4.1(b) depicts the normalized FFT spectra for a healthy motor under 100% load conditions, showcasing the comparison between sampling rates of 2 kHz and 20 kHz. The focus is on the region around the fundamental frequency. Notably, the spectra obtained after interpolation at 20 kHz exhibit a sharper the fundamental frequency component, indicating enhanced frequency resolution. This finding underscores the potential benefits of higher sampling rates in capturing detailed information in motor

current signals.

After the interpolation, the obtained signal is processed using proposed algorithm and the following result are obtained.

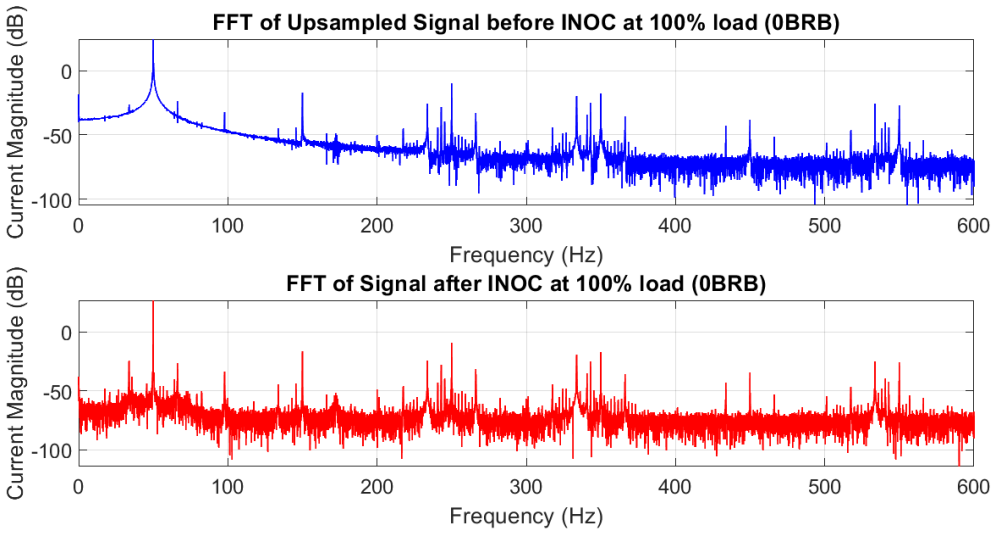

Figure 4.2: FFT plot of the signal before and after counting integral number of cycle

In Figure 4.2, the FFT spectra are presented before and after the application of the proposed methodology, following the interpolation of the signal. The primary focus is on evaluating the impact of the proposed algorithm, which involves discarding starting and ending fractional cycles and ensuring an integral number of cycles. The FFT spectrum after the proposed methodology shows a notable improvement characterized by a reduction in spectral leakage as we can see in the plot.

4.2. Case 2: Motor with one broken rotor bar

The effectiveness of the proposed methodology is study in 1BRB case and following result is obtained. In Figure 4.3 (a), (b), and (c), the FFT plots shows the comparison between signals before and after the proposed algorithm at different loading conditions (100%, 50%, 25% for the scenario of one broken bar.

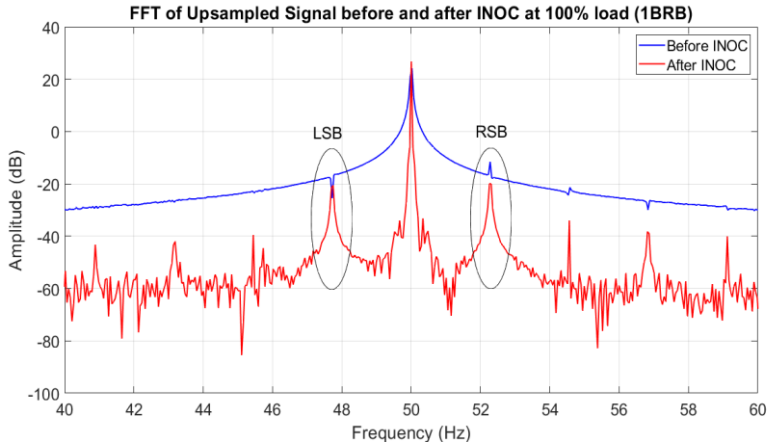

Figure 4.3(a)

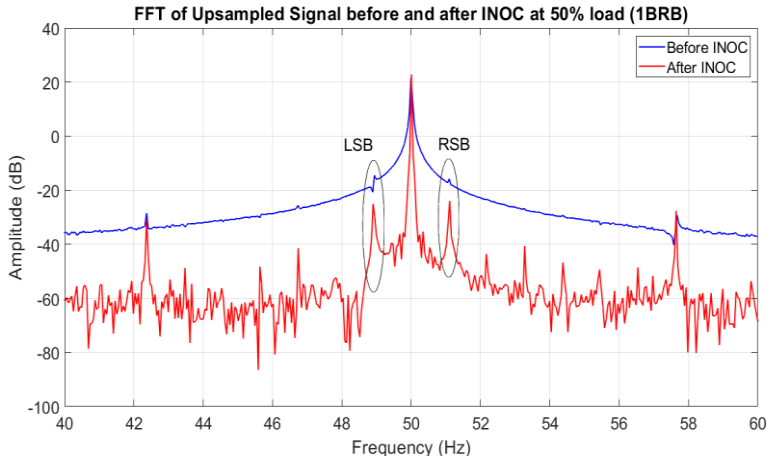

Figure 4.3(b)

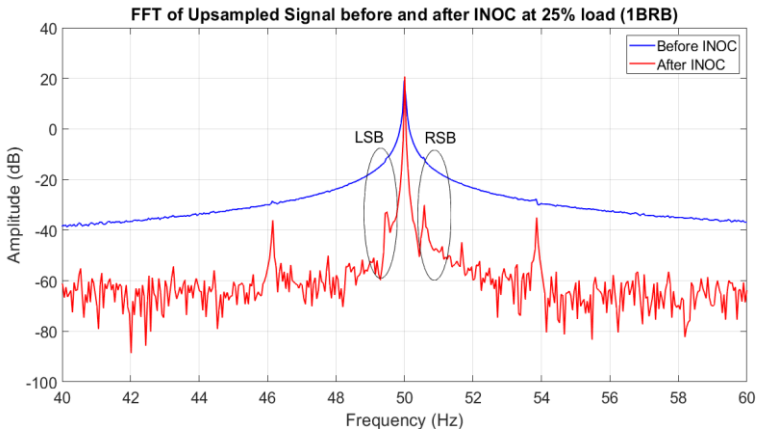

Figure 4.3(c)

Figure 4.3: FFT before and after proposed algorithm for motor with one broken rotor bar, (a) at 100 % load, (b) at 50 % load, (c) at 25 % load

At 100% loading condition, noticeable enhancements are observed in the Left Side Band (LSB) and Right Side Band (RSB) of the fault harmonics after applying the

proposed algorithm. The fault harmonics exhibit sharper peaks, making them distinctly visible. Similarly, at 50% loading condition, the LSB and RSB of fault harmonics, which might be challenging to discern in the raw signal, become more prominent and clearly distinguishable after the application of the proposed algorithm. This improvement contributes to a more precise identification of fault-related features. During the lighter loading condition of 25%, where the slip is substantially low, the LSB and RSB are initially challenging to observe in the raw signal. However, employing the proposed algorithm unveils these components, enabling a clearer distinction. The effectiveness of the algorithm becomes particularly crucial in scenarios where fault-related harmonics are obscured due to low slip, providing valuable insights into the fault diagnosis process.

In summary, the proposed algorithm consistently demonstrates its efficiency across varying loading conditions, significantly improving the visibility and clarity of fault harmonics in the FFT plots. This heightened visibility is pivotal, especially in scenarios with low slip, contributing to more accurate and reliable fault diagnosis.

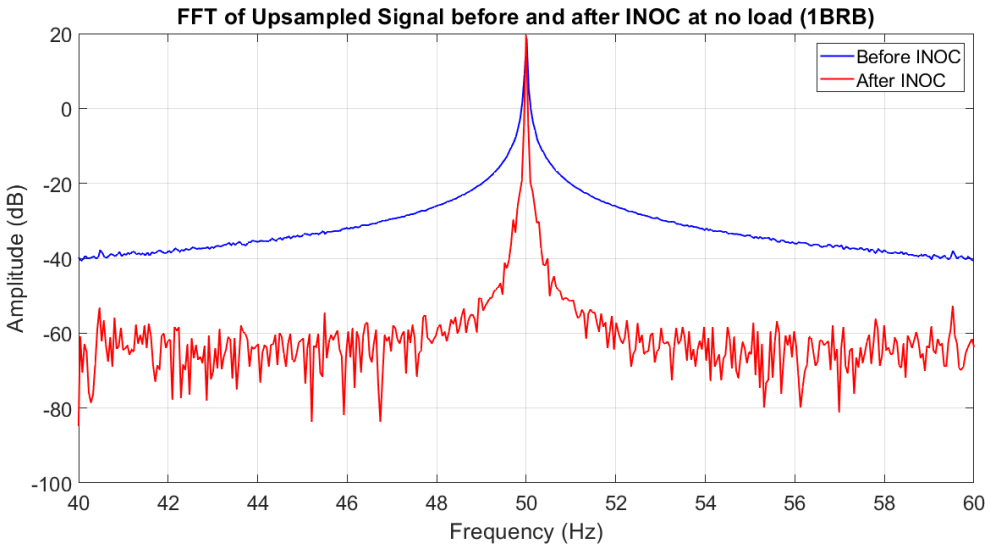

Figure 4.4: FFT of current signal for motor with one broken bar at no load

In Figure 4.4, the FFT plots depict the comparison between signals before and after the proposed algorithm under a no-load condition. Notably, the LSB and RSB of the fault harmonics are challenging to discern in any of the plots. This lack of visibility can be attributed to the extremely low slip at no load, causing the amplitudes of LSB and RSB to be nearly indistinguishable from the fundamental frequency. The phenomenon is particularly pronounced in scenarios where the slip is minimal. The proximity of the

LSB and RSB to the fundamental frequency results in their amplitudes being overshadowed, making them effectively invisible in the raw signal FFT plots. To address this challenge, one potential avenue for further study could involve exploring techniques to attenuate the fundamental component. By reducing the amplitude of the fundamental frequency, the fault-related harmonics, such as LSB and RSB, may become more discernible in the FFT plots, even under conditions of extremely low slip. In conclusion, the difficulties in observing LSB and RSB under a no-load condition underscore the need for innovative approaches to enhance fault visibility in scenarios with minimal slip. Exploring methods to attenuate the fundamental component could be a promising direction for future investigations, potentially improving the efficiency of fault diagnosis in conditions where fault-related harmonics are otherwise challenging to detect.

4.3. Case 3: Motor with two broken rotor bars

The effectiveness of the proposed methodology is study in 1BRB case and following result is obtained. In Figure 4.5 (a), (b), and (c), the FFT plots showcase the comparison between signals before and after the proposed algorithm at different loading conditions (100%, 50%, 25% for the scenario of two broken bar.

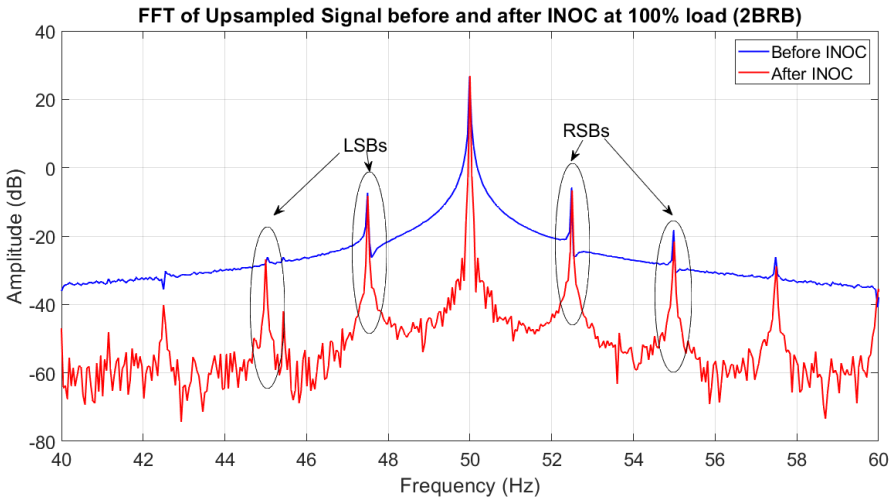

Figure 4.5 (a)

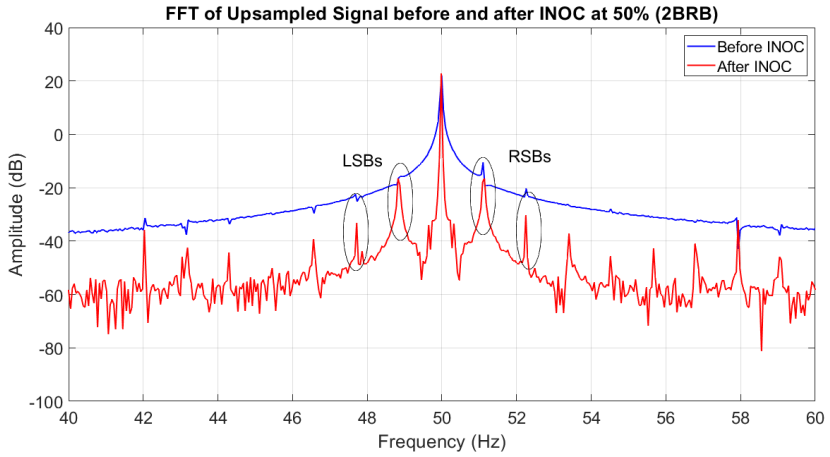

Figure 4.5. (b)

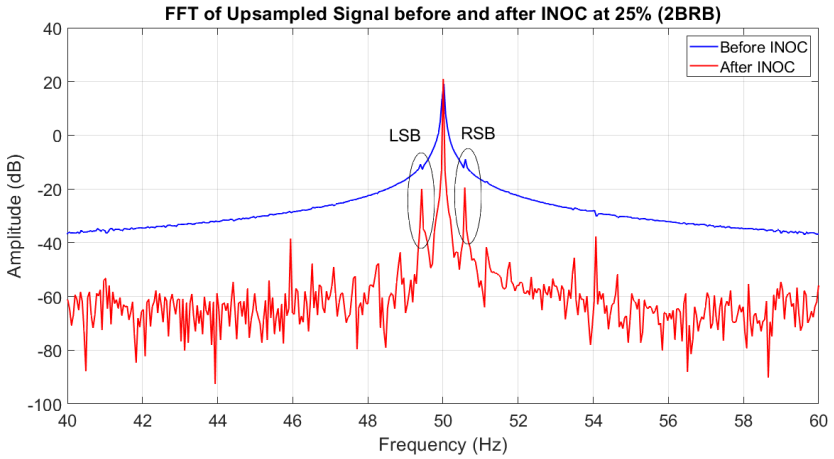

Figure 4.5. (c)

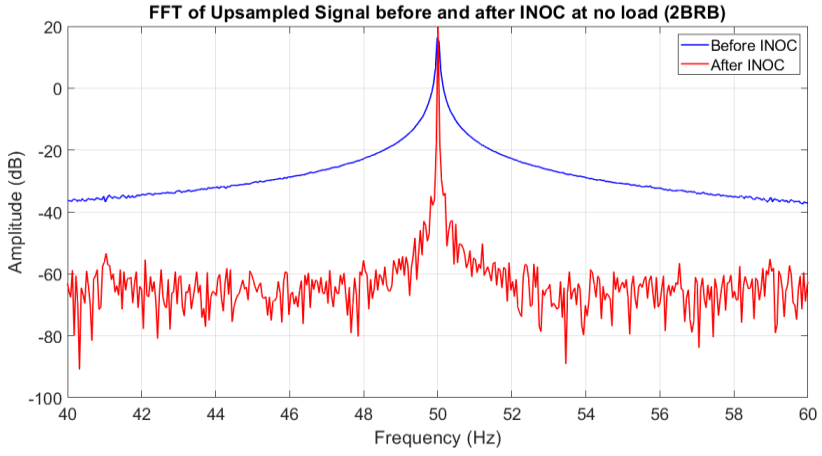

Figure 4.5. (d)

Figure 4.5: FFT before and after proposed algorithm for motor with two broken rotor bars, (a) at 100 % load, (b) at 50 % load, (c) at 25 % load, (d) at no load

Figure 4.5 presents a comprehensive analysis of the FFT results for a two-broken-bar condition across various loading conditions, including 100%, 50%, 25%, and no load. The comparative plots for the spectral content before and after applying the proposed algorithm reveal nuanced insights into the fault detection and signal improvement processes. In subfigure (a) at 100% load, the FFT spectrum showcases distinct enhancements after the application of the proposed algorithm. The Left Side Band (LSB) and Right Side Band (RSB) of fault harmonics become more pronounced and well-defined. This heightened visibility and sharper resolution contribute to a more accurate diagnosis of the two broken bar fault under full load conditions. Transitioning to figure (b) at 50% load, a similar trend is observed. The LSB and RSB, though less prominent than at full load, are significantly clearer post-application of the proposed algorithm. This highlights the algorithm's effectiveness in distinguishing fault harmonics even under moderate loading conditions. In figure (c) at 25% load, where fault harmonics are typically less discernible, the proposed algorithm once again proves instrumental. It facilitates the identification of LSB and RSB, offering a notable improvement in fault diagnosis during light loading conditions. Similarly, the problem associated with no load condition is also seen for two broken bars condition. These results collectively affirm the versatility and efficacy of the proposed algorithm in optimizing fault diagnosis across varying loading conditions for a two-broken-bar fault scenario. The algorithm's consistent ability to improve fault visibility, even under challenging low-load scenarios, underscores its potential for practical implementation in real-world applications.

4.4. Comparison of FFT Results after INOC for Different Sampling Rates

In this section, we delve into a comparative analysis of the Fast Fourier Transform (FFT) spectra obtained from signals processed through the Integral Number of Cycles (INOC) methodology at different sampling rates. Specifically, we will first examine the effectiveness of the INOC methodology at a sampling rate of 2 kHz. By comparing the FFT spectra before and after applying the INOC method, we aim to demonstrate that even at a lower sampling rate of 2 kHz, the INOC method produces satisfactory results, effectively identifying fault-related harmonics and minimizing spectral leakage.

Following this, we will extend our analysis to include a higher sampling rate of 20 kHz. By comparing the FFT spectra after applying INOC at both 2 kHz and 20 kHz, we will highlight the improvements in spectral resolution and the reduction in spectral leakage

achieved with a higher sampling rate. This comparison aims to underscore the advantages of a 20 kHz sampling rate, showing how it provides a clearer and more detailed representation of the signal, thereby enhancing the accuracy and reliability of fault diagnosis.

Figure 4.6 presents the FFT spectra before and after applying the Integral

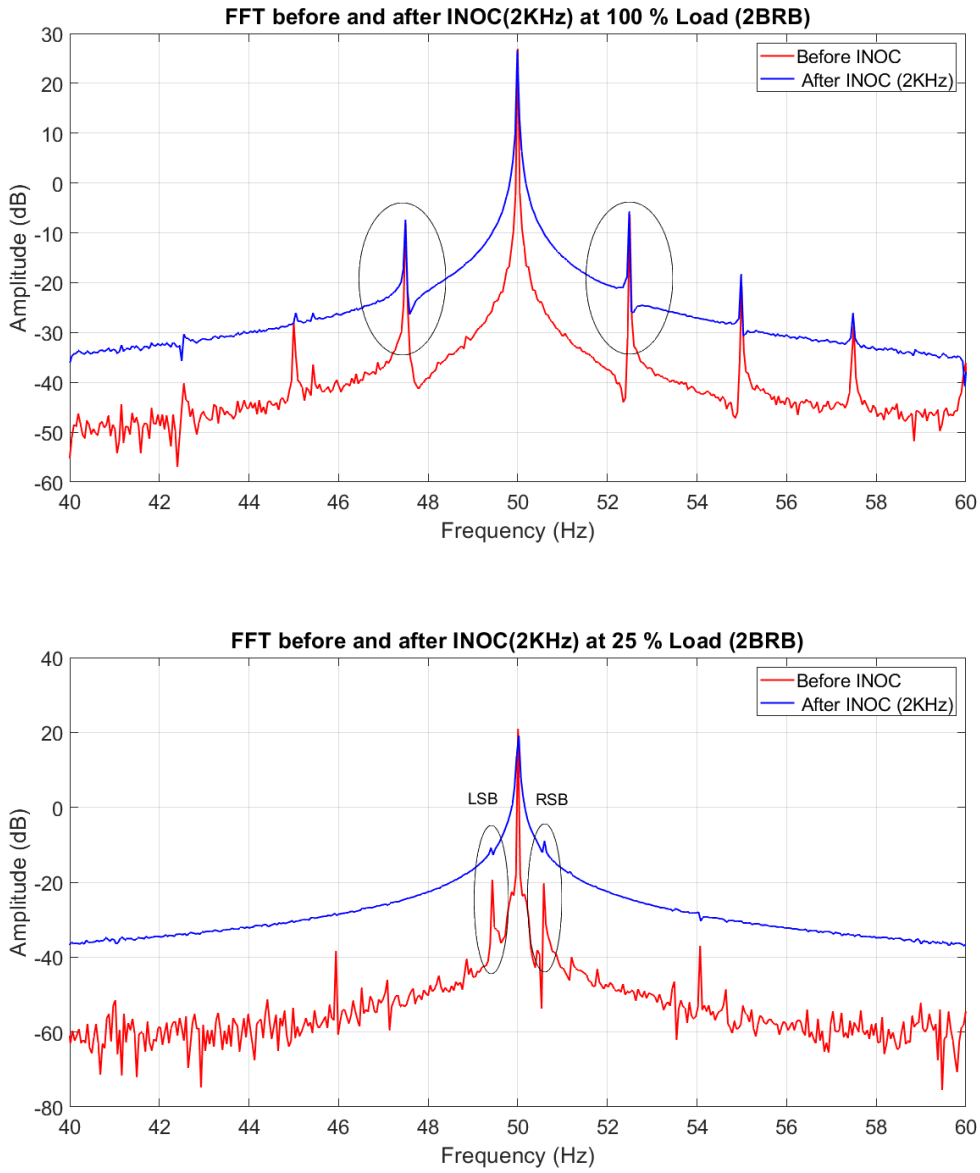

Figure 4.6: FFT before and after INOC(at 2KHz sampling rate) for motor with two broken rotor bars, at 100 % load, and at 25 % load,

Number of Cycles (INOC) methodology for a motor with two broken rotor bars, comparing the results at a 2 kHz sampling rate under two different loading conditions: 100% load and 25% load.

The comparison illustrates that even at the lower sampling rate of 2 kHz, the application of the INOC method significantly enhances the clarity and sharpness of the frequency spectrum. Before applying INOC, the FFT spectrum exhibits noticeable spectral leakage, with fault harmonics appearing broader and less distinct. However, after applying the INOC method, there is a marked reduction in spectral leakage, resulting in fault harmonics that are more sharply defined and easier to distinguish. This improvement is evident at both 100% and 25% load conditions, demonstrating the effectiveness of the INOC method in improving fault detection even at a lower sampling rate. Despite these improvements, the figure also indicates that the results at 2 kHz can be further enhanced through upsampling.

Comparison between the spectrum of signal at sampling rates of 2 KHz and 20 KHz after counting integral no of cycle is discussed later in this section. Figure 4.7 presents a comparative analysis of the frequency spectra obtained after applying the Integral Number of Cycles (INOC) methodology to signals sampled at 2 kHz and 20 kHz under different loading conditions for a motor with one broken rotor bar (1BRB). The spectra derived from the 2 kHz sampling rate exhibit clear fault-related harmonics, indicating that even at a lower sampling rate, the INOC methodology can effectively identify key spectral features associated with motor faults. However, when comparing these results to those obtained from the 20 kHz sampling rate, several improvements become apparent.

At 20 kHz, the spectra show significantly reduced spectral leakage, resulting in sharper and more well-defined peaks. This higher resolution allows for a more precise identification of the Left Side Band (LSB) and Right Side Band (RSB) harmonics associated with the broken rotor bar fault. The higher sampling rate leads to less spectral leakage, which means that the amplitude of side frequencies is significantly reduced in the 20 kHz condition compared to the 2 kHz condition. This reduction in spectral leakage provides a clearer distinction between the fundamental and fault-related harmonics, thereby improving the accuracy and reliability of the fault diagnosis.

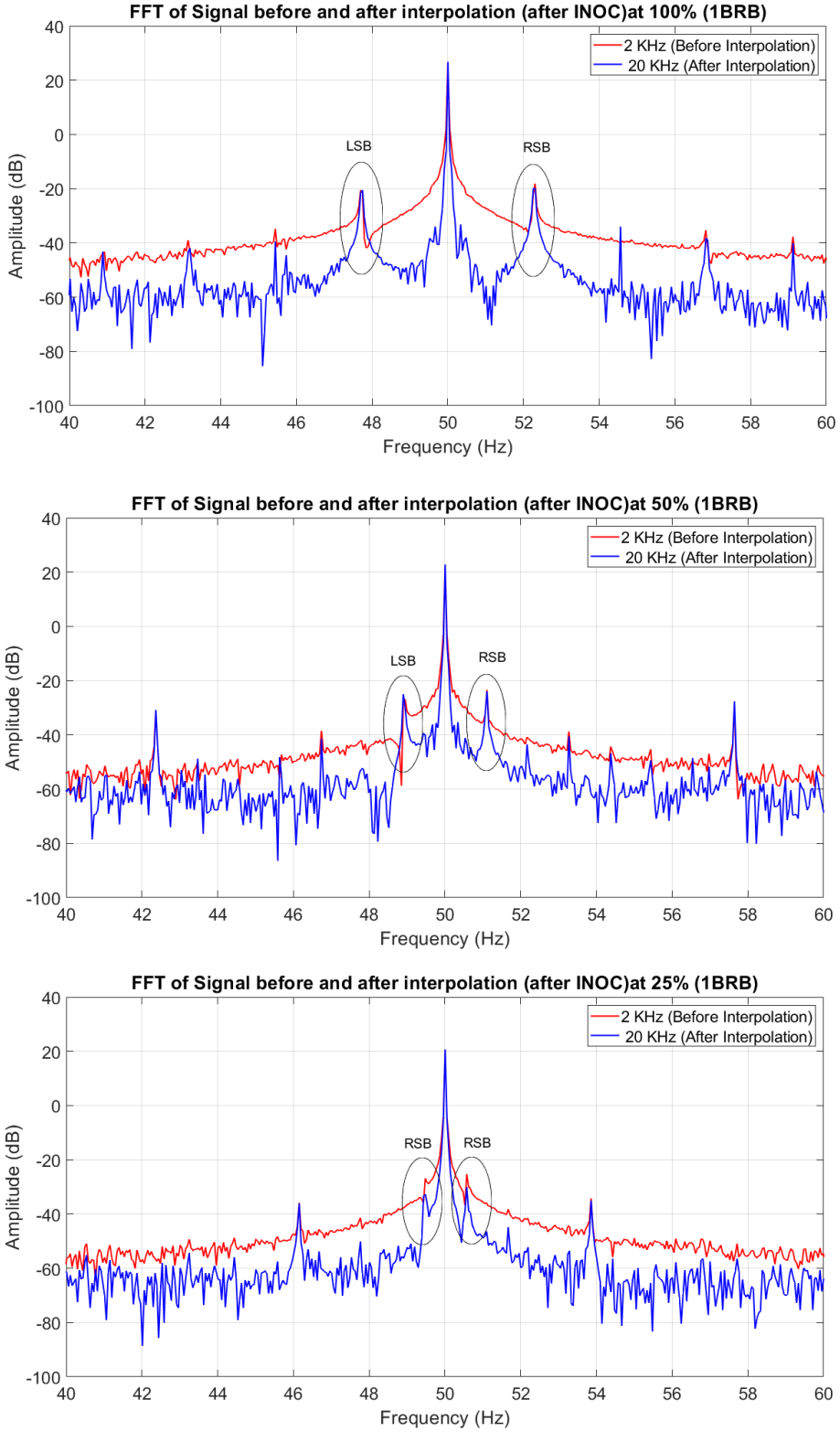

Figure 4.7: :Comparison of spectrum obtained by FFT after INOC between signal with sampling rate of 2 KHz and 20 KHz at different loading condition for 1BRB condition.

The enhanced clarity and reduced noise in the 20 kHz spectra facilitate a more accurate and reliable fault diagnosis, particularly under varying load conditions. This comparison underscores the benefits of using a higher sampling rate for detailed signal analysis, as it leads to more distinct and interpretable spectral features, thereby improving the overall diagnostic capability of the INOC methodology. Despite the fact of the advantages of high sampling rate. while using 2 KHz sampling rate, the memory requirement is almost one tenth than the memory requirement for 20 KHz sampling rate data and calculation complexity is also much lesser as no upsample is required and FFT is done for small size data.

4.5. Comparison between FFT with Hann window and FFT after counting INOC

The FFT with Hann window after multi-rate resampling and before resampling as described in the methodology is shown in Figure 4.8 below. Where the 20 KHz original sampling rate is resampled to 16384 Hz with the Window length is fixed at N = 131072. After resampling the frequency resolution changes from 0.1526 Hz to 0.125 Hz and M from 327.6 to 400 making it the exact integer. From Figure 4.8 (a) (b) and (c) we can see that after making the fundamental frequency equal to exact integer multiple of frequency resolution there has been increase in the sharpness of the frequency spectrum, mainly for the low load condition the fault harmonics are seen more clearly.

Figure 4.8.(a)

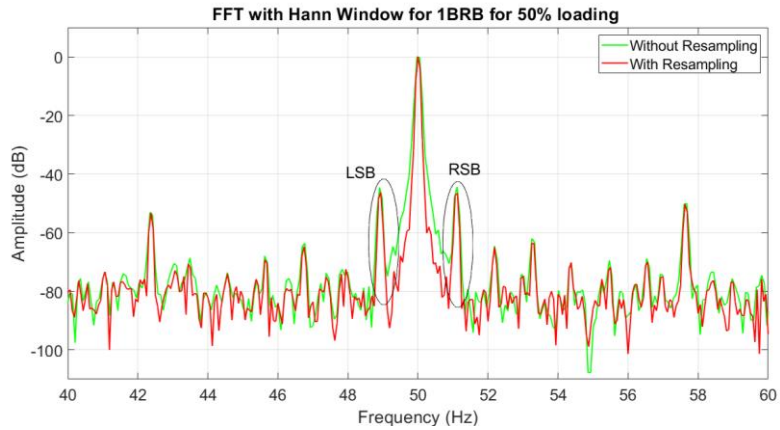

Figure 4.8. (b)

Figure 4.8. (c)

Figure 4.8: FFT with Hann window before and after resampling for motor with one broken rotor bars, (a) at 100 % load, (b) at 50 % load, (c) at 25 % load,

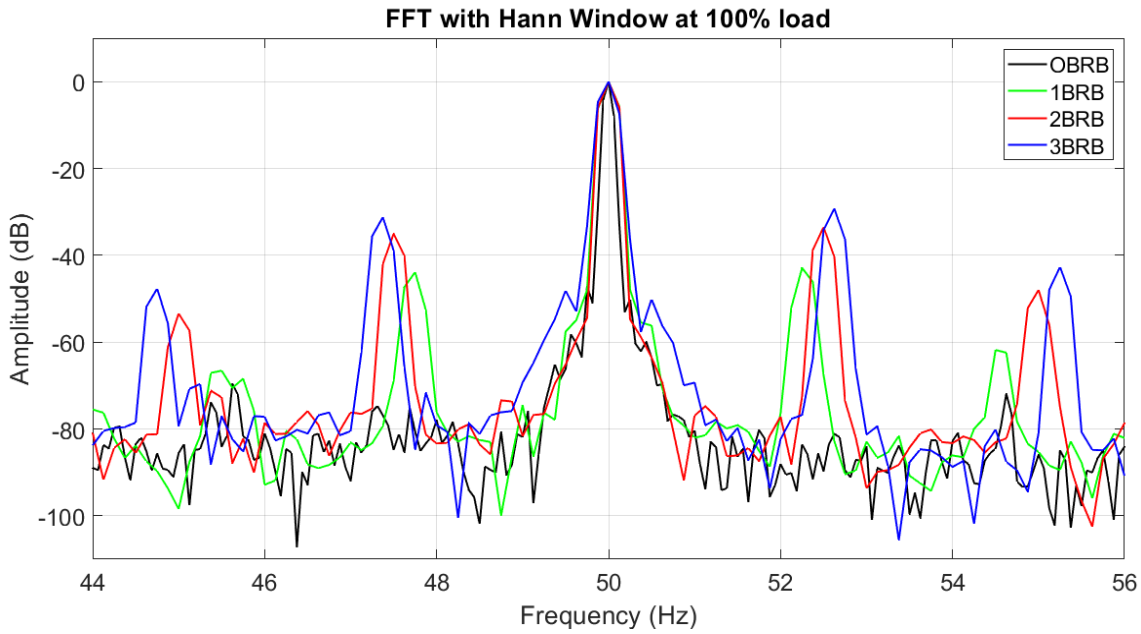

Figure 4.9(a)

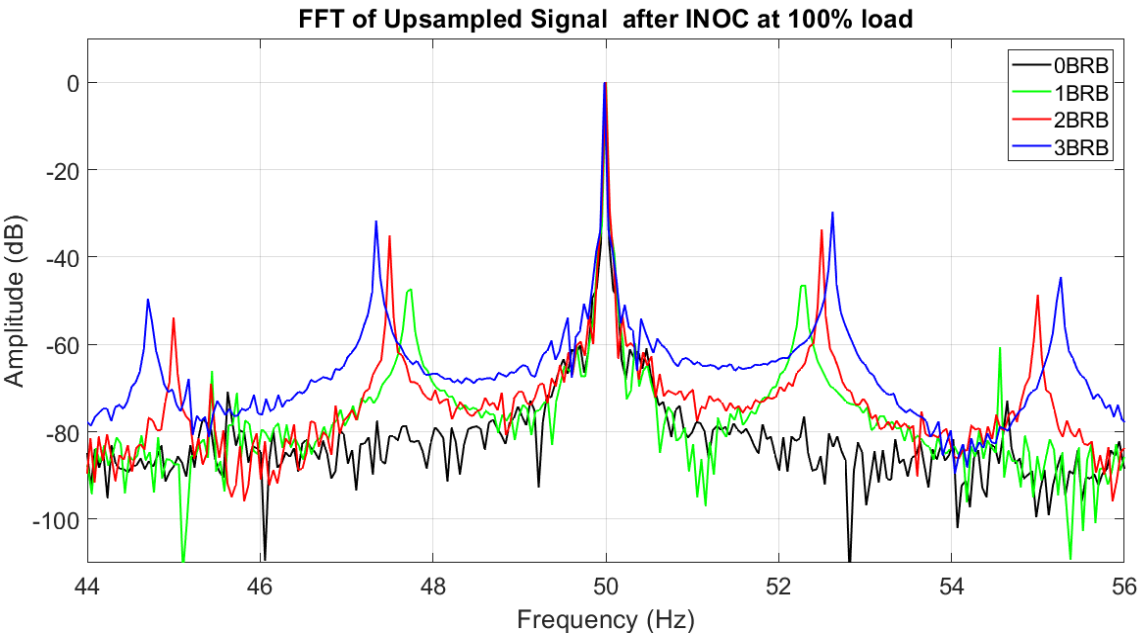

Figure 4.9 (b)

Figure 4.9:Comparison of spectrum obtained by (a) FFT with Hann Window and (b) FFT after INOC for motor at 100% loading condition

Figure 4.9(a) displays the frequency spectrum obtained by applying the Fast Fourier Transform (FFT) with a Hann window after multirate resampling. In contrast, Figure (b) showcases the frequency spectrum using FFT after counting integral no of cycle using proposed algorithm, the proposed algorithm detailed earlier. Both plots focus on

the 100% loading condition and present the spectral content for varying degrees of broken rotor bars (BRB), ranging from 0 to 3.

In Figure 4.9(a), the spectrum obtained with the Hann window exhibits sharpness, attributed to the windowing technique. However, in figure (b), the spectrum obtained after applying the INOC algorithm, despite potential differences in sharpness, delivers satisfactory results. The primary focus lies in the spectrum's ability to effectively capture and represent the fault harmonics associated with different BRB scenarios.

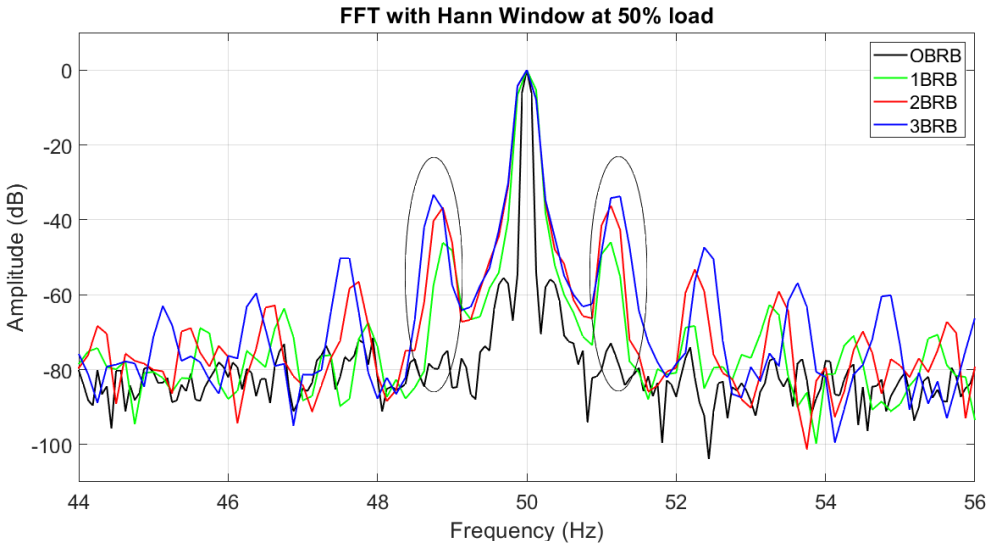

(a)

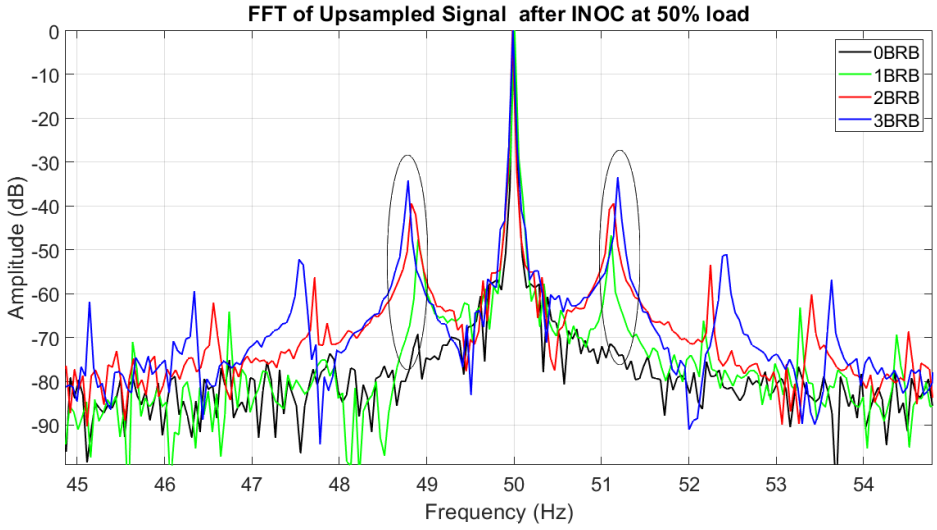

(b)

Figure 4.10::Comparison of spectrum obtained by (a) FFT with Hann Window and (b) FFT after proposed techniques (after INOC) for motor at 50% loading condition

Figure 4.10 continues the comparison, focusing on the 50% loading condition. The

spectrum obtained with the Hann window in Figure 4.10(a) again shows the benefits of windowing, with sharp and clear fault harmonics. However, the spectrum obtained after applying the INOC algorithm in Figure 4.10(b) demonstrates a similar level of clarity and definition. The proposed methodology effectively captures the fault harmonics, ensuring that they are distinguishable and accurately represented. Even at this reduced load, where spectral leakage can be more prominent, the INOC method provides robust and reliable results. This indicates that the proposed algorithm maintains its diagnostic capabilities across different loading conditions, ensuring consistent fault detection performance.

In Figure 4.11, the comparison is extended to the 25% loading condition, where the challenges of spectral leakage and noise are more significant due to lower energy levels in the signal. The spectrum obtained with the Hann window in Figure (a) shows sharp peaks corresponding to the fault harmonics. Interestingly, Figure (b) demonstrates that the INOC algorithm performs exceptionally well even at this low load condition. The fault harmonics are clearly distinguishable, and there is a noticeable reduction in spectral leakage compared to the raw FFT. This improvement is critical for fault diagnosis at low loads, where traditional methods might struggle. The proposed methodology's effectiveness in enhancing the spectral content, even in challenging conditions, highlights its potential as a superior diagnostic tool.

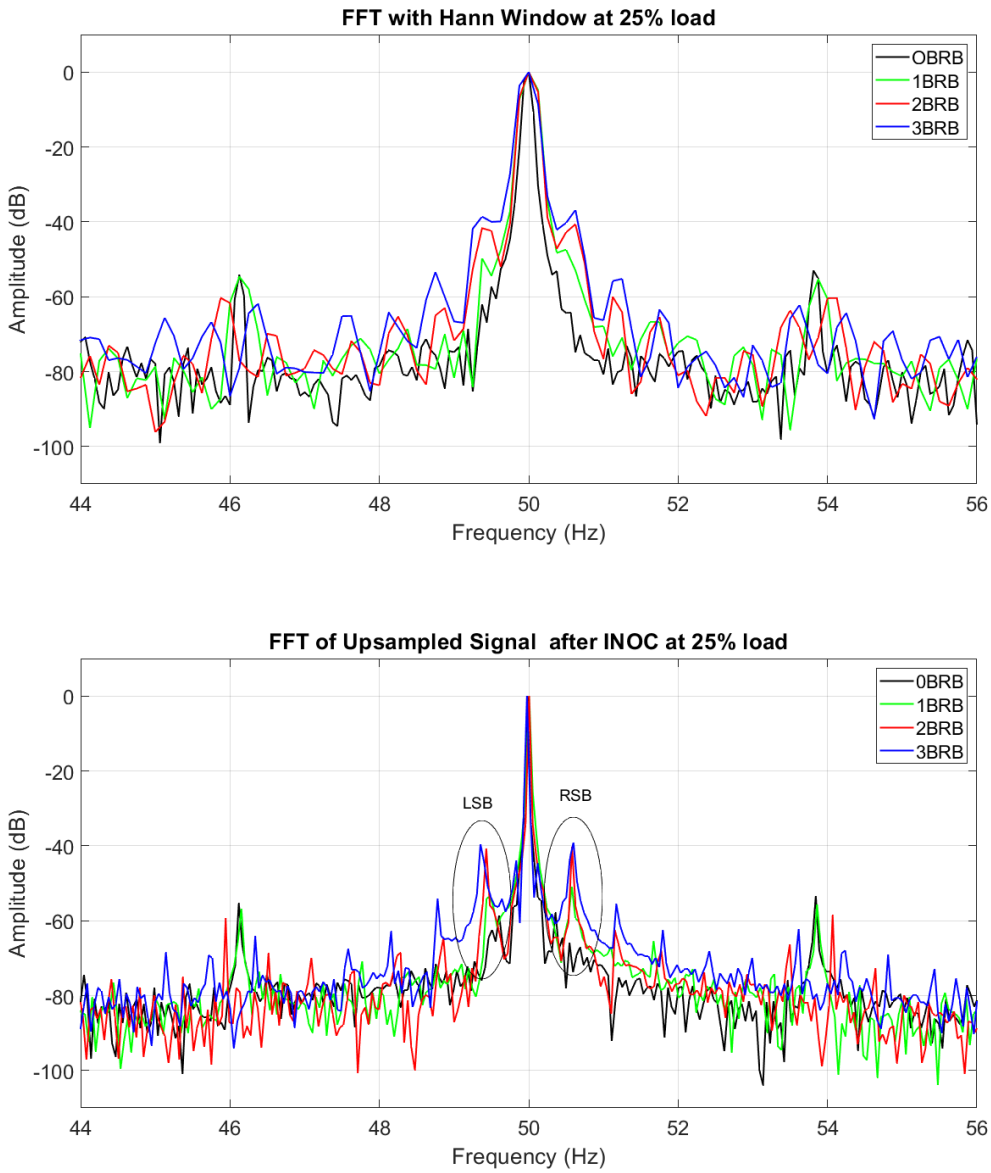

Figure 4.11: Comparison of spectrum obtained by FFT with Hann Window and FFT after proposed techniques (after INOC) for motor at 25% loading condition

Upon close examination, it is observed that the amplitude of fault harmonics for 0 BRB, 1 BRB, 2 BRB, and 3 BRB conditions remains consistent in the spectrum produced by the proposed algorithm. This uniformity in fault harmonic amplitudes suggests that the proposed algorithm successfully retains the diagnostic information associated with varying degrees of rotor bar faults, even without the need for a Hann window. While the spectrum obtained with the Hann window may appear sharper, the satisfactory performance of the proposed algorithm is evident in its ability to reliably distinguish and represent fault harmonics. This robustness across different BRB conditions underscores the potential of the proposed algorithm as a viable alternative to

conventional windowing techniques, offering a balance between simplicity and diagnostic efficacy.

Overall, the comparison across Figures 4.9, 4.10, and 4.11 indicates that the proposed INOC method provides consistently satisfactory results across different loading conditions. While the Hann window technique offers sharp spectra, the INOC algorithm not only matches but often surpasses its performance, particularly in reducing spectral leakage and enhancing fault harmonic visibility. This makes the proposed method a compelling alternative for motor fault diagnosis, ensuring reliable and accurate detection of rotor bar faults under various operational scenarios.

4.6. Comparative Analysis of Fault Harmonics

Here, a detailed comparative analysis of fault harmonics under various loading conditions (100%, 75%, 50%, and 25%) using two signal processing techniques is presented: FFT with a Hann Window and FFT after applying the proposed integral number of cycles (INOC) algorithm. This analysis focuses on the detection and representation of Left Sideband (LSB) and Right Sideband (RSB) frequencies and their corresponding amplitudes. Table 5 compares fault harmonics at various loading conditions (100%, 75%, 50%, and 25%) using FFT with a Hann Window and FFT with the proposed INOC algorithm. The analysis highlights LSB and RSB frequencies and their amplitudes for different broken rotor bar (BRB) scenarios.

At 100% loading, for 1BRB, the Hann Window method shows LSB and RSB at 47.75 Hz and 52.25 Hz, with amplitudes of -43.88 dB and -42.92 dB. The INOC algorithm refines these to 47.75 Hz and 52.26 Hz, with amplitudes of -47.34 dB and -46.64 dB. Hence the amplitude of the fault harmonics remains consistent after purposed methodology. Similarly, for 75%, 50%, and 25% loading, similar refinements are observed, with the INOC algorithm consistently providing precise frequency and amplitude measurements. The result is further analyzed with the help of the plot of the amplitude of fault harmonics at different loading conditions.

Table 4.1: Fault Harmonics and their Amplitude for FFT with Hann window and FFT after INOC (20 KHz)

% Loading	Condition	Fault Harmonics							
		FFT with Hann Window				FFT after INOC (20 KHz)			
		LSB (Hz)	Amplitude (dB)	RSB (Hz)	Amplitude (dB)	LSB (Hz)	Amplitude (dB)	RSB (Hz)	Amplitude(dB)
100	1BRB	47.75	-43.8778	52.25	-42.9221	47.7468	-47.338	52.2575	-46.6423
	2BRB	47.5	-38.9157	52.5	-34.1958	47.4982	-35.1378	52.498	-33.6556
	3BRB	47.375	-31.213	52.625	-29.2476	47.34	-31.704	52.623	-29.7692
75	1BRB	48.125	-44.378	51.875	-43.7549	48.1164	-44.3256	51.8807	-43.7879
	2BRB	48.25	-35.0824	51.75	-34.5113	48.25	-38.4716	51.75	-37.884
	3BRB	48.375	-31.6944	51.625	-30.5494	48.3501	-31.8378	51.6412	-30.7523
50	1BRB	48.875	-46.1259	51.125	-45.9675	48.9009	-47.6503	51.1106	-46.6437
	2BRB	48.875	-37.1502	51.125	-36.2036	48.8249	-39.4516	51.1384	-39.4065
	3BRB	48.75	-33.3071	51.25	-33.7378	48.787	-34.2167	51.1856	-33.4516
25	1BRB	49.375	-49.7105	50.625	-47.4229	49.3538	-53.3865	50.5984	-50.8692
	2BRB	49.375	-41.7217	50.625	-40.6461	49.4316	-40.7812	50.5789	-40.3396
	3BRB	49.375	-38.6137	50.625	-36.8411	49.382	-34.7342	50.5769	-35.2314

Figure 4.12 illustrates the amplitudes of the Left Sideband (LSB) and Right Sideband (RSB) frequencies for various broken rotor bar (BRB) conditions and loading percentages, comparing these amplitudes with the healthy condition.

The findings from this figure reveal several key observations:

1. **Increase in Amplitude with More Broken Bars:** As the number of broken rotor bars increases, the amplitude of the fault harmonics also increases. This trend is evident across all loading conditions, indicating a clear correlation between the severity of rotor bar damage and the magnitude of the fault harmonic amplitudes.
2. **Loading Impact on Amplitude Difference:** With increasing load, the difference in amplitude between the healthy condition and the broken bar conditions becomes more pronounced. This suggests that higher loading exacerbates the effects of rotor faults, making the detection of broken bars more distinguishable at higher loads.

3. **Consistency Across FFT Methods:** The amplitude of the fault harmonics remains consistent when comparing FFT with INOC to FFT with Hann Window. Both methods

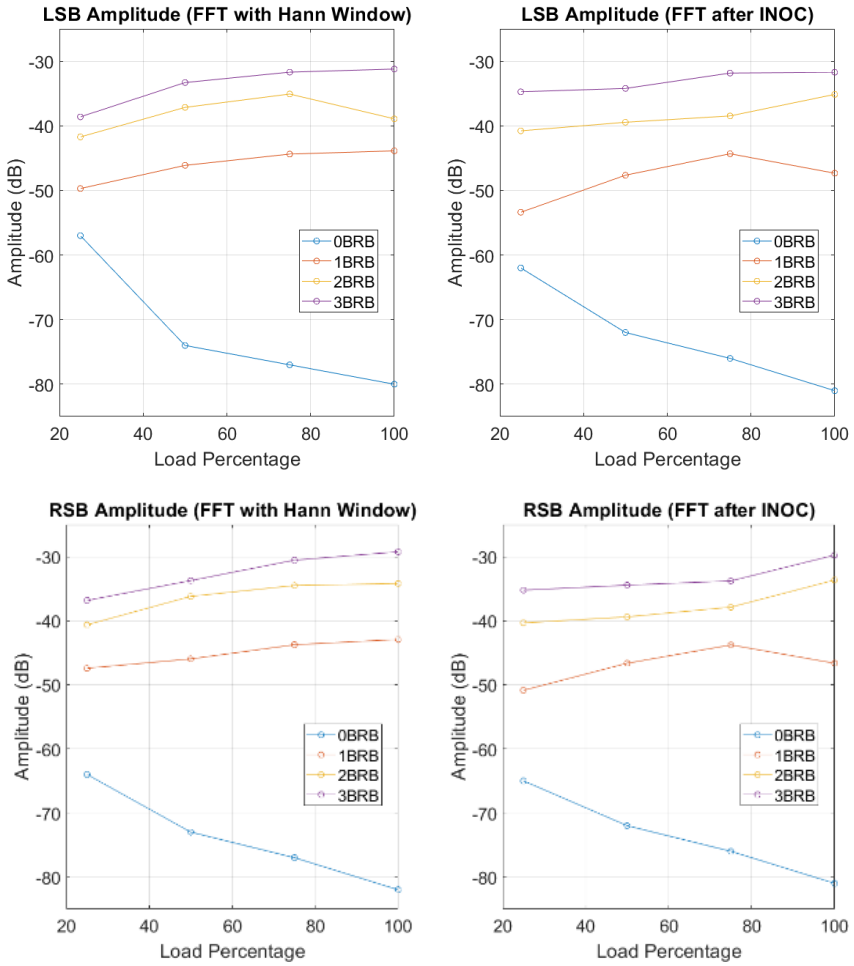

Figure 4.12:: Comparison of LSB and RSB amplitude of fault harmonics at different BRB condition for different loading conditions.

yield similar results in terms of amplitude values, highlighting that the proposed INOC algorithm achieves comparable accuracy to the traditional Hann Window method. However, it is noted that the FFT after INOC provides a sharper spectral representation, which can be beneficial for more precise fault detection.

These findings underscore the reliability and robustness of the INOC algorithm in detecting rotor bar faults under various loading conditions. The ability to maintain consistent amplitude measurements across different signal processing techniques reinforces the validity of using INOC for practical fault diagnosis in induction motors.

Table 4.2: Fault Harmonics and their Amplitude FFT after INOC (2 KHz)

% Loading	Condition	Fault Harmonics			
		FFT after INOC (2KHz)			
		LSB (Hz)	Amplitude (dB)	RSB (Hz)	Amplitude(dB)
100	1BRB	47.6967	-47.0682	52.3033	-44.7828
	2BRB	47.4977	-35.0069	52.4975	-33.3616
	3BRB	47.343	-31.8174	52.6241	-29.7566
75	1BRB	48.3496	-44.7015	51.6407	-43.6314
	2BRB	48.2498	-38.5044	51.6928	-38.0162
	3BRB	48.1554	-31.9392	51.8797	-30.5814
50	1BRB	48.948	-49.9749	51.1096	-46.0181
	2BRB	48,824	-39.2563	51.1375	-38.6967
	3BRB	48.7863	-34.109	51.1899	-33.7551
25	1BRB	49.4814	-47.4613	50.5757	-46.0859
	2BRB	49.4311	-40.2471	50.5784	-41.1813
	3BRB	49.3558	-40.8628	50.5984	-38.6382

Table 4.2 presents the fault harmonics and their amplitudes for FFT analysis after applying the INOC method at a low sampling rate of 2 kHz, compared to the high sampling rate of 20 kHz used in Table 4.1. The findings reveal that the lower sampling rate method can still accurately detect the fault frequencies, as both the LSB and RSB frequencies remain consistent across both tables. For example, at 100% loading, the LSB frequencies for 1BRB, 2BRB, and 3BRB are approximately 47.70 Hz, 47.50 Hz, and 47.34 Hz, respectively, in both tables. The RSB frequencies show similar consistency. While there are minor amplitude discrepancies, with the amplitudes recorded at 2 kHz slightly lower in some cases, the general trend remains the same: the amplitude of both LSB and RSB increases with the number of broken rotor bars. This trend is consistent across different loading conditions, demonstrating the reliability of the low sampling rate method.

In Figure 4.13 we can see that for 2KHz signal there is one misinterpretation for 25% loading condition as the amplitude for 2BRB condition is higher than 3 BRB condition which can lead to false identification during fault diagnosis. As we also can see that the fault amplitude difference between healthy and broken bar condition is less for 2 KHz signal which means less sharpness of the signal and higher spectral leakage. So it already shown that the quality of spectrum can be increased by improving the initial low sampling rate data by multi-rate resampling. Even if the data is up sampled it is

still acquired at low sampling rate. Hence the lower sampling rate offers significant advantages in data efficiency, reducing memory requirements and processing power for data acquisition without significantly compromising fault detection accuracy. This makes the method highly suitable for real-time analysis, minimizing data loss and processing delays, and proving that low sampling rate data acquisition can be a viable and advantageous approach for condition monitoring of electrical machines.

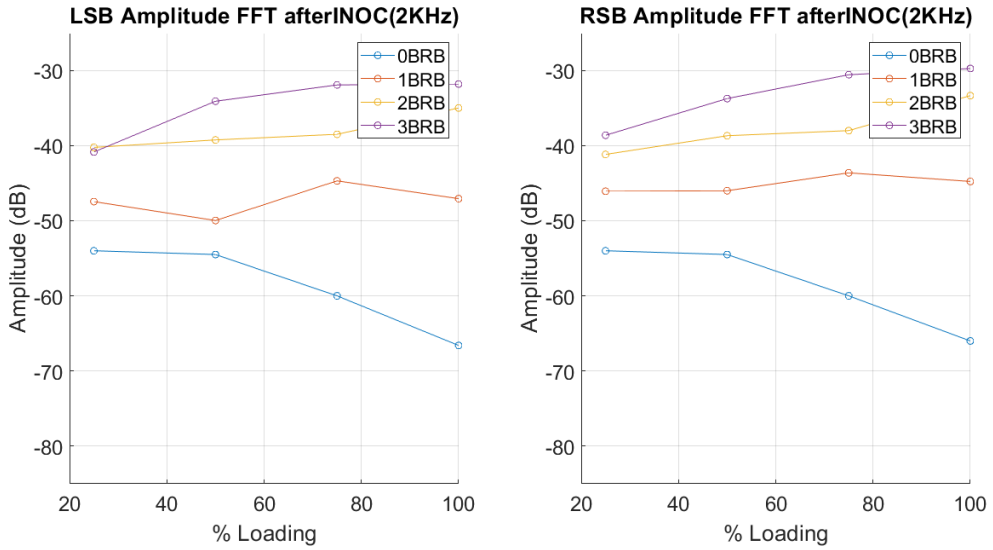

Figure 4.13: LSB and RSB fault harmonics amplitude for FFT after INOC (2KHz).

To further validate these results, we compare the LSB and RSB frequencies obtained through both techniques with the theoretical fault harmonics. The theoretical fault harmonics are calculated using the formula $f_{BR} = f_s \pm 2ksf_s$ where k=1 for first fault harmonics and s is the slip of the motor. These theoretical values serve as a benchmark to assess the accuracy and effectiveness of the FFT with Hann Window and the proposed INOC algorithm.

Table 4.3: Theoretical LSB and RSB frequency at different loading conditions.

Loading Condition	**Slip**	**LSB (Hz)**	**RSB (Hz)**
25%	0.25×0.0267=0.0067	49.33	50.67
50%	0.50×0.0267=0.0133	48.67	51.33
75%	0.75×0.0267=0.0200	48	52
100%	1.00×0.0267=0.0267	47.33	52.67

When comparing these results with the theoretical values provided in Table 4.3, we observe that the theoretical LSB and RSB frequencies for different loading conditions align closely with the observed values from both techniques. However, slight discrepancies are present due to practical factors such as measurement noise, signal processing imperfections, and inherent differences between theoretical models and real-world data. The theoretical values in Table 4.1 serve as a benchmark for evaluating the accuracy of the observed frequencies. For instance, at 100% loading, the theoretical LSB and RSB frequencies are 47.33 Hz and 52.67 Hz, respectively, which are close to the observed values but not exact. These slight differences highlight the real-world challenges in fault diagnosis and the importance of refined algorithms like INOC to minimize errors.

The minor differences between LSB and RSB frequencies in the observed data can be attributed to several factors, including the asymmetric distribution of the fault harmonics and variations in load conditions affecting the rotor dynamics. Additionally, the inherent characteristics of the Hann Window method and the proposed INOC algorithm influence the precision of the frequency estimation, resulting in minor deviations from the theoretical values. Overall, the comparison underscores that the INOC algorithm provides similar consistent results to the FFT with Hann Window, but the spectrum appears sharper. This sharper spectral representation is crucial for reliable fault detection and analysis in induction motors under varying operational conditions.

4.7. Spectrum Analysis at no load condition.

As the fault harmonics depends on the slip of the motor and at no load and very low load condition the slip for the motor is very low which results the fault harmonics very near to the fundamental conditions. There is a probability that the fault harmonics components get dominated by the fundamental components which makes it difficult to distinguish the BRBs conditions in the induction motor. Here in this section the no load condition is analyzed using different conditions mentioned in the methodology.

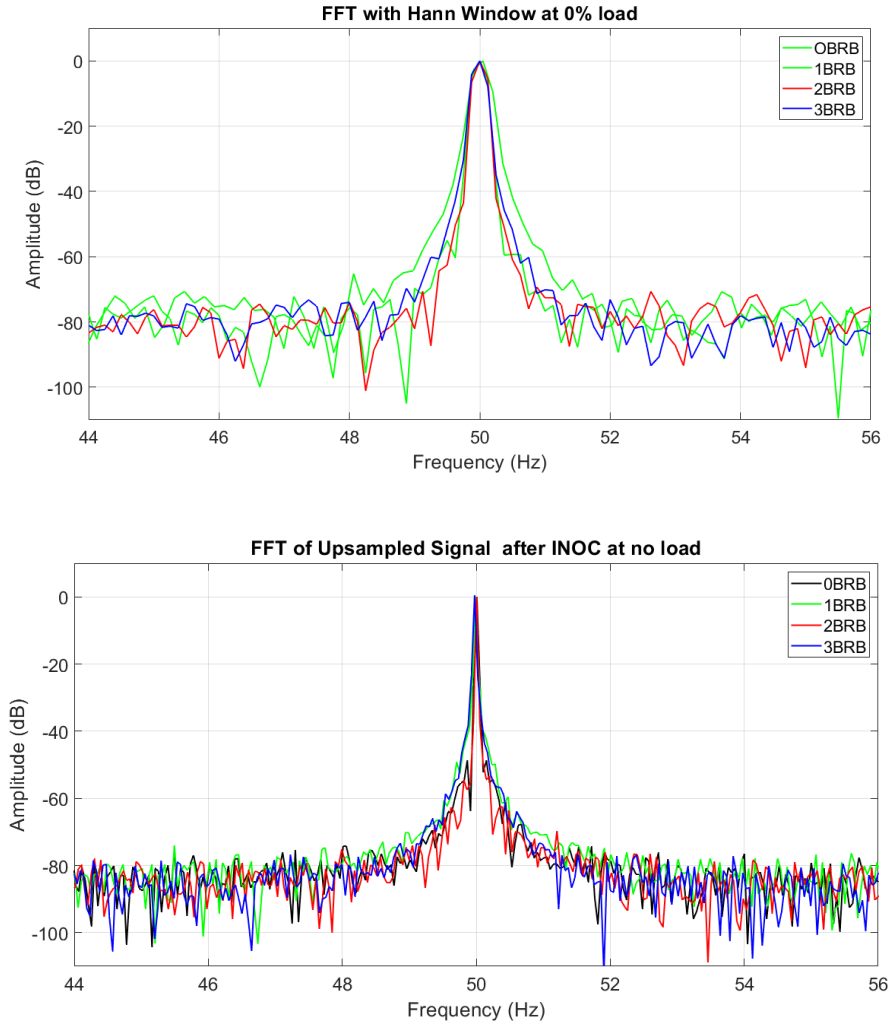

Figure 4.14:Spectrum analysis at no load condition

In Figure 4.14, the spectrum analysis at no load condition is presented, comparing different broken rotor bar (BRB) conditions: 0BRB (healthy), 1BRB, 2BRB, and 3BRB using both FFT with Hann Window and FFT after applying the Integral Number of Cycles (INOC) algorithm.

At no load, the slip of the motor is very low, making it difficult to distinguish between healthy and faulty rotor conditions. The LSB and RSB fault harmonics for 1BRB, 2BRB, and 3BRB are not discernible from the healthy condition (0BRB). Both FFT with Hann Window and FFT after INOC show similar spectral characteristics, with no distinct fault harmonics standing out from the baseline noise. This analysis reveals the challenge of fault detection at very low load conditions. However, our study successfully distinguishes fault harmonics at load conditions as low as 25%. For no load conditions, new diagnostic methods may be required to effectively detect rotor faults.

CHAPTER FIVE: CONCLUSION

In the current era, where efficient predictive maintenance holds paramount importance, our research addresses critical challenges associated with traditional condition monitoring techniques for electrical machines. We emphasize the need for reliable fault detection methods, especially for broken rotor bar faults in induction motors. By introducing Integral Number of Cycles (INOC) into the Fast Fourier Transform (FFT) process, we have significantly enhanced the spectral analysis of machine signals.

Summary of Key Findings:

1. **Low Sampling Rate Feasibility**: The data acquisition was performed at a low sampling rate of 2 kHz, which proved sufficient for detecting fault harmonics in induction motors. This approach significantly reduces the risk of data loss, minimizes memory requirements, and facilitates real-time analysis, making it advantageous for practical implementation.
2. **FFT with Hann Window vs. FFT after INOC**: Comparative analysis was conducted between traditional FFT with Hann Window and FFT after applying the Integral Number of Cycles (INOC) algorithm. Our findings demonstrated that FFT after INOC not only provided results consistent with FFT with Hann Window but also produced sharper spectral representations without the need for windowing techniques.
3. **Fault Detection Across Different Loading Conditions**: The analysis was carried out under various loading conditions (25%, 50%, 75%, and 100%). It was observed that as the number of broken rotor bars increased, the amplitude of the fault harmonics also increased. Furthermore, the difference between the healthy condition and faulty conditions became more pronounced with higher loading. Even at a 25% loading condition, fault harmonics were distinguishable, highlighting the robustness of the INOC algorithm in low-load scenarios.
4. **Challenges at No Load Condition**: At no load, distinguishing between healthy and faulty conditions was challenging due to the very low slip of the motor. Both signal processing techniques struggled to identify fault harmonics under these conditions, suggesting the need for alternative methods or additional diagnostic tools for no load condition monitoring.

5. **Memory and Data Efficiency**: Using a low sampling rate of 2 kHz reduces the amount of data generated, thereby decreasing storage requirements and improving data handling efficiency:
6. **Practical Implementation** The elimination of the need for windowing techniques simplifies the implementation of the FFT after INOC algorithm, making it a practical choice for real-world condition monitoring systems.

This research has successfully demonstrated that signal spectrum-based condition monitoring of electrical machines can be effectively achieved using low sampling rates. The FFT after INOC algorithm, with its sharp spectral outputs and consistency across different loading conditions, offers a reliable alternative to traditional methods. Despite challenges at no load conditions, the overall findings affirm the potential of this approach for enhancing the reliability and efficiency of motor condition monitoring in various industrial applications.

Hence, the main objective of our research to perform signal spectrum analysis at a low sampling rate is fulfilled by obtaining data at a sampling rate of 2 kHz. Even with FFT performed at 2 kHz, we achieved satisfactory results. The quality of the spectrum can be further improved by interpolating the data to 20 kHz. This demonstrates that low sampling rates can effectively be used for condition monitoring of electrical machines, offering significant advantages such as reduced memory requirements and processing power, while maintaining accuracy in fault detection. In addition to achieving the main objective, our research successfully eliminates the need for windowing functions in signal spectrum analysis, simplifying the analytical process while maintaining precision. Furthermore, the analysis conducted across different loading conditions consistently yielded satisfactory results, underscoring the robustness and versatility of the proposed methodology. Future work may focus on developing complementary techniques to address the limitations observed at very low load conditions.

CHAPTER SIX: RECOMMENDATIONS

Future work could focus on enhancing fault detection at no load conditions by developing new methods. Expanding the analysis to other fault types and various electrical machines would improve the methodology's generalizability. Investigating different low sampling rates could help optimize the balance between data resolution and storage requirements. Validating the proposed algorithm in real-time industrial settings would ensure practical feasibility and computational efficiency. Comparing the INOC method with other advanced signal processing techniques could identify potential improvements. Finally, integrating machine learning algorithms could enhance predictive maintenance and automated fault diagnosis.

REFERENCES

[1] R. Li and D. He, "Rotational machine health monitoring and fault detection using EMD-based acoustic emission feature quantification," *IEEE Transactions on Instrumentation and Measurement,* vol. 61, p. 990–1001, 2012.

[2] L. Menozzi, "Technologies for machine condition monitoring," *SDEMPED 2011 Tutorials,* p. 5–8, 2011.

[3] P. Tavner, Condition monitoring of rotating electrical machines, vol. 56, IET, 2008.

[4] B. Asad, T. Vaimann, A. Belahcen, A. Kallaste, A. Rassõlkin and M. N. Iqbal, "The cluster computation-based hybrid FEM–analytical model of induction motor for fault diagnostics," *Applied Sciences,* vol. 10, p. 7572, 2020.

[5] B. Asad, T. Vaimann, A. Belahcen, A. Kallaste, A. Rassõlkin and M. N. Iqbal, "Broken rotor bar fault detection of the grid and inverter-fed induction motor by effective attenuation of the fundamental component," *IET Electric Power Applications,* vol. 13, p. 2005–2014, 2019.

[6] S. Owatchaiphong, "Design Concept of Low Cost Measurement for Motor Current Signature Analysis," in *2018 Third International Conference on Engineering Science and Innovative Technology (ESIT),* 2018.

[7] M. Benbouzid, "Bibliography on induction motors faults detection and diagnosis," *IEEE Transactions on Energy Conversion,* vol. 14, p. 1065–1074, 1999.

[8] B. Akin, S. Choi, U. Orguner and H. A. Toliyat, "A simple real-time fault signature monitoring tool for motor-drive-embedded fault diagnosis systems," *IEEE Transactions on Industrial Electronics,* vol. 58, p. 1990–2001, 2010.

[9] B. Kim, K. Lee, J. Yang, S. B. Lee, E. J. Wiedenbrug and M. R. Shah, "Automated detection of rotor faults for inverter-fed induction machines under standstill

conditions," *IEEE Transactions on Industry Applications,* vol. 47, p. 55–64, 2010.

[10] B. Asad, T. Vaimann, A. Belahcen and A. Kallaste, "Broken rotor bar fault diagnostic of inverter fed induction motor using FFT, Hilbert and Park's vector approach," in *2018 XIII International Conference on Electrical Machines (ICEM)*, 2018.

[11] M. Z. Ali, M. N. S. K. Shabbir, X. Liang, Y. Zhang and T. Hu, "Machine learning-based fault diagnosis for single-and multi-faults in induction motors using measured stator currents and vibration signals," *IEEE Transactions on Industry Applications,* vol. 55, p. 2378–2391, 2019.

[12] B. Asad, T. Vaimann, A. Kallaste, A. Rassõlkin, A. Belahcen and M. N. Iqbal, "Improving legibility of motor current spectrum for broken rotor bars fault diagnostics," *The Scientific Journal of Riga Technical University-Electrical, Control and Communication Engineering,* vol. 15, p. 1–8, 2019.

[13] R. Jaros, R. Byrtus, J. Dohnal, L. Danys, J. Baros, J. Koziorek, P. Zmij and R. Martinek, "Advanced signal processing methods for condition monitoring," *Archives of Computational Methods in Engineering,* vol. 30, p. 1553–1577, 2023.

[14] B. Asad, H. A. Raja, T. Vaimann, A. Kallaste, R. Pomarnacki and V. K. Hyunh, "A Current Spectrum-Based Algorithm for Fault Detection of Electrical Machines Using Low-Power Data Acquisition Devices," *Electronics,* vol. 12, p. 1746, 2023.

[15] R. de Jesus Romero-Troncoso, "Multirate signal processing to improve FFT-based analysis for detecting faults in induction motors," *IEEE Transactions on industrial informatics,* vol. 13, p. 1291–1300, 2016.

[16] H. A. Raja, K. Kudelina, B. Asad, T. Vaimann, A. Kallaste, A. Rassõlkin and H. V. Khang, "Signal Spectrum-Based Machine Learning Approach for Fault Prediction and Maintenance of Electrical Machines," *Energies,* vol. 15, p. 9507, 2022.

[17] J. CusidÓCusido, L. Romeral, J. A. Ortega, J. A. Rosero and A. G. Espinosa,

"Fault detection in induction machines using power spectral density in wavelet decomposition," *IEEE Transactions on Industrial Electronics,* vol. 55, p. 633–643, 2008.

[18] A. Sapena-Bano, M. Pineda-Sanchez, R. Puche-Panadero, J. Perez-Cruz, J. Roger-Folch, M. Riera-Guasp and J. Martinez-Roman, "Harmonic order tracking analysis: A novel method for fault diagnosis in induction machines," *IEEE transactions on energy conversion,* vol. 30, p. 833–841, 2015.

[19] A. Sapena-Bano, J. Burriel-Valencia, M. Pineda-Sanchez, R. Puche-Panadero and M. Riera-Guasp, "The harmonic order tracking analysis method for the fault diagnosis in induction motors under time-varying conditions," *IEEE Transactions on Energy Conversion,* vol. 32, p. 244–256, 2016.

[20] J. Milimonfared, H. M. Kelk, S. Nandi, A. D. Minassians and H. A. Toliyat, "A novel approach for broken-rotor-bar detection in cage induction motors," *IEEE Transactions on Industry Applications,* vol. 35, p. 1000–1006, 1999.

[21] S. A. a. M. M. a. o. Taher, "A novel technique for rotor bar failure detection in single-cage induction motor using FEM and MATLAB/SIMULINK," *Mathematical Problems in Engineering,* vol. 2011, 2011.

[22] N. a. S. S. a. T. A. Bessous, "A detailed study of the spectral content in the stator current of asynchronous machines under broken rotor bar faults using MCSA technique," *2018 6th International Conference on Control Engineering \& Information Technology (CEIT),* pp. 1--8, 2018.

[23] K. Kudelina, B. Asad, T. Vaimann, A. Rassõlkin, A. Kallaste and H. V. Khang, "Methods of condition monitoring and fault detection for electrical machines," *Energies,* vol. 14, p. 7459, 2021.

[24] J. Martinez, A. Belahcen and A. Muetze, "Analysis of the vibration magnitude of an induction motor with different numbers of broken bars," *IEEE transactions on industry applications,* vol. 53, p. 2711–2720, 2017.

[25] M. Rigoni, N. Sadowski, N. J. Batistela, J. P. A. Bastos, S. L. Nau and A. Kost, "Detection and analysis of rotor faults in induction motors by the measurement of the stray magnetic flux," *Journal of Microwaves, Optoelectronics and Electromagnetic Applications,* vol. 11, p. 68–80, 2012.

[26] C. Harlişca, L. Szabó, L. Frosini and A. Albini, "Diagnosis of rolling bearings faults in electric machines through stray magnetic flux monitoring," in *2013 8TH International Symposium on Advanced Topics in Electrical Engineering (Atee)*, 2013.

[27] N. M. Elkasabgy, A. R. Eastham and G. E. Dawson, "Detection of broken bars in the cage rotor on an induction machine," *IEEE transactions on industry applications,* vol. 28, p. 165–171, 1992.

[28] A. Belahcen, J. Martinez and T. Vaimann, "Comprehensive computations of the response of faulty cage induction machines," in *2014 International Conference on Electrical Machines (ICEM)*, 2014.

[29] B. Asad, T. Vaimann, A. Belahcen, A. Kallaste and A. Rassõlkin, "Rotor fault diagnostic of inverter fed induction motor using frequency Analysis," in *2019 IEEE 12th International Symposium on Diagnostics for Electrical Machines, Power Electronics and Drives (SDEMPED)*, 2019.

APPENDIX A: PUBLICATION

Pulchowk Campus
Institute of Engineering
Tribhuvan University

ASHISH PAUDEL <078mspse004.ashish@pcampus.edu.np>

[IOEGC15] Editor Decision

1 message

IOEGC15 Publication Committee <conference-noreply@ioe.edu.np> Mon, Jun 10, 2024 at 8:36 AM
To: Ashish Paudel <078mspse004.ashish@pcampus.edu.np>, Nava Raj Karki <nrkarki@ioe.edu.np>, Basanta Kumar Gautam <basanta.gautam@pcampus.edu.np>

Ashish Paudel; Nava Raj Karki, Basanta Kumar Gautam:

We have reached a decision regarding your submission to 15th IOE Graduate Conference, "Impact of Sampling Rate Variations on Signal Spectrum Based Fault Diagnosis of Induction Motor".

Our decision is to: **Accept Submission**

[*This email is auto-generated from 15th IOE Graduate Conference web portal*]

IOE Graduate Conference
[Placeholder for Publication Information]

Impact of Sampling Rate Variations on Signal Spectrum Based Fault Diagnosis of Induction Motor

Ashish Paudel [a], Nava Raj Karki [b], Basanta Kumar Gautam[c]

[a,b,c] *Department of Electrical Engineering, Pulchowk Campus, Institute of Engineering, Tribhuvan University, Nepal*
[a] 078mspse004.ashish@pcampus.edu.np,

Abstract
The investigation looks into how sampling rate variations affect induction motors fault diagnosis based on signal spectrum analysis. Modern companies depend heavily on induction motors, but they can develop mechanical and electrical problems that, if not found quickly, can result in significant financial loss and downtime. Fault identification relies heavily on signal processing techniques, particularly Motor Current Signature Analysis (MCSA). The Fast Fourier Transform (FFT) technique for frequency spectrum analysis is the main topic of this work. This study investigates how the FFT spectrum is affected when sample rates are changed using decimation and interpolation techniques, with a focus on the diagnosis of broken rotor bar (BRB) problems in induction machines. The methodology involves determining acquisition parameters, calculating the required sampling rate, performing interpolation and decimation, and applying FFT with proper window functions. Spectral leakage, a common issue in FFT-based techniques, is addressed using Hann window function. Experimental results are presented for a healthy motor, a motor with one BRB at different loading conditions, and a motor with BRB at no load. The study compares original sampling rates of 20 KHz obtained from experimental setup in laboratory and with resampled sampling rates using purposed methodology. The findings emphasize the importance of choosing an appropriate sampling rate based on fault visibility and computational efficiency.

Keywords
Induction Motor, Fault Diagnosis, Broken Rotor Bar, Fourier Transform

1. Introduction

Since the second industrial revolution started, induction motors have become really important in modern industries. They are used in various ways, like generating power and in things we use every day. For example, they play a crucial role in renewable energy sources like wind power plants. Induction motors also help convert electrical energy into mechanical energy, driving many industries and impacting a country's economy. They're widely used in everyday things like electric vehicles, fans, water pumps, and more. While there are other machines that can do the same job, induction motors are popular because they are simple, efficient, and easy to fix. They use a lot of electricity, about half of the total generated worldwide [1]. These equipment feature moving parts, which makes them prone to malfunctions. There are two primary categories of these issues: mechanical and electrical. Electrical faults, which include inconsistent voltage, phase drop, short circuits between turns, and grounding issues, are mostly associated with the stator. Most faults are mechanical in nature, and include things like broken end rings, rotor bars, and damaged bearings, as well as faulty part positioning. These faults are directly or indirectly related with each other and are degenerative in nature. Hence, it is very important to detect them at an incipient stage in order to avoid extensive economic loss and time-consuming repair processes.

Electrical machine diagnostics today employ a variety of faults detection techniques. Advanced signal processing methods are essential for predicting engine maintenance requirements. There has been a discernible shift in the development of digital technology during the last few years. This change makes it possible to use reasonably priced hardware platforms that have efficient data processing capabilities. These hardware platforms can be used to enhance the performance of real-time diagnostic

systems in addition to identifying instant messaging malfunctions [2]. Determining the best methods for signal processing is crucial to determining whether induction motor (IM) maintenance is required. Predicting maintenance can cut down on expenses and repair time for instant messaging. Scholars across the globe are investigating several approaches to accomplish this. Spectral Kurtosis (SK), Park's Vector Approach (PVA), Wavelet Transform (WT), Empirical Mode Decomposition (EMD), Singular Value Decomposition (SVD), Hilbert Transform (HT), Wigner-Ville Distribution (WVD), Principal Component Analysis (PCA), Independent Component Analysis (ICA), and Kalman Filter (KF)are just a few of the widely used techniques.

The major goal of any signal processing techniques was to identify any new frequencies in the overall signal of the system that would point to a fault. In order to locate and save the tiny, delicate, and crucial information linked to faults, researchers spent a great deal of time developing signal processing systems. They concentrated on improving the spectrum resolution under both steady state and dynamic conditions. This was a shared objective to enhance our ability to recognize and address machine problems. A significant number of AI-based research are also being done and number is increasing. The accuracy and maturity of AI- algorithm depends on the data size [3]. Thanks to different mathematical modeling like Finite Element Method (FEM) [4], data collection is possible using simulation. But the collection of large set of data at higher sampling rate for better spectral resolution and accuracy is issue for both simulation and experimental set up. It comes with calculation complexity and memory storage requirement. The data acquisition at higher sampling rate in real time diagnosis of fault in industrial machine is also not economical [3]. This is not a parameter that can be easily adjusted [5].

This paper describes how to change the initial sample frequency by decimation and resampling, and it shows how change in sampling rates affect the signal's frequency spectrum for diagnosing broken rotor bar (BRB) faults in induction motor in various scenarios.

2. Background

Motor current signature analysis (MCSA) based fault diagnostic techniques are being extensively used in research, because these techniques are mostly noninvasive in nature and require simple measurements [6]. After the current measurement, there comes an entire domain of signal processing techniques to estimate the nature and the severity of the fault. The fast Fourier transform (FFT) one of the most utilized signal processing methods for these purposes [7]. In this paper FFT is used to study the frequency spectrum of current signal obtained from the experimental set up of healthy motor and induction motor with broken rotor bars.

Depending on the defect's severity, each failure causes a different frequency and modulation index in the stator current. The geometric and electrical parameters of the rotor and stator determine the mathematical representation of these fault frequencies. Early detection of a broken bar is crucial because when one breaks, the subsequent bars are subjected to increased thermal stress, which may lead to their failure. Certain harmonics in the frequency spectrum are produced by these faults [8].

$$f_{br} = f_s \pm 2ksf_s \tag{1}$$

$$f_{br} = [(k/p)(1-s) \pm s]f_s \tag{2}$$

where k = 1,2,3....., f_s is supply frequency, s is the slip and p is the no of poles pairs of the machine. The fault-related harmonics are denoted as the left side band (LSB) and right side band (RSB). These fault harmonics can be buried under fundamental frequency spectrum because of their dependency on slip. These problem is more severe for the motor running under the low load condition.

2.1 Fast Fourier Transform

In numerous scientific fields, the Fast Fourier Transform (FFT), is a useful tool. It assists in splitting an erratic signal into distinct components known as sinusoids. Amplitude is the term used to describe the frequency and size of these sinusoids. These sinusoids typically get smaller in size as we examine across a range of frequencies. The foundational component is the most significant. This process is represented mathematically by formulas known as the discrete Fourier transform (DFT) and its inverse.

$$X_k = \sum_{n=0}^{N-1} x_n e^{-\frac{j2\pi kn}{N}},\ k = 0,1,2,...(N-1) \tag{3}$$

$$x_n = \frac{1}{N}\sum_{n=0}^{N-1} X_n e^{-\frac{j2\pi kn}{N}},\ k = 0,1,2,...(N-1) \tag{4}$$

where k is the current frequency, N is the number of samples, n is the current sample, x_n is the signal value at time n, and X_k is the DFT resulting bin.

2.2 Interpolation

The technique of guessing or projecting values between current data points in a signal is known as interpolation. Put otherwise, it's a technique for adding to or filling in the blanks within a range where the initial signal values are known. There are various interpolation methods, and the method of choice is determined by the particular needs and signal characteristics. Spline interpolation, cubic interpolation, and linear interpolation are a few popular interpolation techniques.

If the interpolation is done by n times, the new frequency of sampling is increased by f_r=nf_s along with the bandwidth (BW). Where, f_r is new resampled frequency and f_s is original sampling frequency.

2.3 Decimation

The process of decimation involves lowering the amount of samples in a signal, usually by deleting some of the samples on purpose. It is the interpolation process done in reverse. Decimation is the process of lowering the number of samples to get a lower sampling rate, whereas interpolation entails predicting values between current samples to increase the number of data points.

Mathematically, The relationship between the initial sampling rate (f_s) and the new sampling rate (f_d) following decimation can be expressed as f_d=$\frac{f_s}{m}$ along with the bandwidth (BW). where m is the decimation factor which can be chosen according to the requirement.

Hence, using interpolation and decimation we can perform fractional resampling as:

$$f_r = \frac{n}{m} f_s \tag{5}$$

And the frequency resolution $\nabla f = \frac{f_s}{N}$, where f_s is sampling frequency and N is the no of input data samples. From equation (5) the value of n and m or N can also be choose in such a way that the fundamental frequency will be equal to the exact integer multiple frequency resolution which also helps in reducing the effect of spectral leakages for FFT based techniques [5].

2.4 Methodology

The following is the intended methodology for altering the signal's sample rate through the use of intended techniques:

1. Find the acquisitions parameters like sampling frequency f_s, fundamental frequency of the signal and sampling length N.
2. Determine the required sampling rate f_r.
3. Using Eqn.5, determine the integer value of n and m and proceed to interpolate n times.
4. Decimate the interpolated signal m times to get the required sampling rate.
5. Find the FFT of the resampled signals using proper window functions (Hann Window).

When spectral energy from a signal spills into nearby frequency bins, it's called leakage. Because window functions taper the signal towards the endpoints, they assist reduce leakage. For this, functions like Hann and Hamming are frequently employed. For this research Hann window function is used to perform the signal analysis. Spectral leakage is one of the major problem of FFT techniques which has not been sufficiently studied [9]. When two characteristic frequencies are positioned closely together, spectral leakage becomes more noticeable because the spurious components of both frequencies interfere with each other. This condition frequently occurs when broken rotor bar detection occurs in induction motors, especially when the motor is operating with a low mechanical load, changing loads, or low-frequency load oscillations. In these cases, the fault's characteristic frequency nearly matches with the main frequency. The spectral leakage caused by the main frequency interferes with spectral components that are close together, like those linked to broken rotor bars, if the main frequency does not match specific requirements, as stated by equation (5). While total reduction of leakage is not possible, it can be reduced by employing a Hann window [5].

3. Experimental Results and Discussion

The motor input current of healthy motor and motor with one and two broken rotor bars(BRB) at different

loading conditions were obtained from experimental setup. The motor bars were drilled to simulate the BRB. Initially the current data is obtained at sampling rate of 20kHz initially. Following cases are studied at different sampling rates.

3.1 Case A: Healthy motor at 100% of the rated load.

The first case of the study is done for healthy motor at 100% of the rated load. The motor is fed from the grid supply of frequency 50Hz. The original sampling frequency is 20 KHz and study is done at 4 kHz and 32 kHz using purposed method. The original data length is 4×10^6. The nearest power of two to the data length is N= 2^{18} 262144. Figure 1 gives the FFT of the healthy motor using Hann window and without using Hann window at sampling rates of 2 KHz (m=10, n=1), 20 KHz (original) and 32 KHz (m=5, n=8). The spectrum is zoomed at near the fundamental region. The resampled sampling frequencies are calculated using purposed method. The window length for 2 KHz and 32 KHz is 16384 and 524288. It shows that the spectrum of the signal using Hann window is sharper than without using. It also shows that the more the sampling rate sharper the spectrum of the signal.

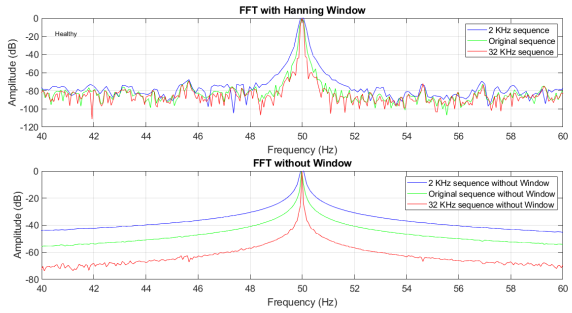

Figure 1: FFT spectrum of original and resampled data signal for healthy motor at 100% of rated load with and without Hann window

3.2 Case B: Motor with 1 BRB at 25%, 50% and 100% of the rated load.

The second case study is done for Induction motor with one broken bars for three loading condition: 25%, 50% and 100% of the rated load. The study is done for original sampling rate (20KHz), 2 KHz and 32 KHz. The window lengths are same as previous case. Figure 2 shows the FFT spectrum for different sampling rate at different loading condition. The spectrums are zoomed in region of interest which is near fundamental frequency as the fault bands due to broken bar can be seen near fundamental frequency. In Figure 2a for 25% loading condition, without window we cannot see any LSB or RSB. With Hann window the LSB and RSB for the sampling rate of 20 KHz and 32 KHz are clearly shown but these components are shown in a sharper way can be easily distinguish but we cannot see LSB of 2 KHz sequence clearly. Similarly Figure 2b shows the spectrogram of the signal for 50% loading condition and Figure 2c shows the spectrogram of the signal for 100% loading condition. Figure 3 shows comparing spectra obtained at 32 KHz and 50 KHz sampling rates reveals minimal enhancements in spectrum sharpness despite increased computational time and memory usage. Utilizing MATLAB 2023b with an Intel Core i5 processor, simulation times for 25% loading condition with 1 BRB were 0.54181 seconds and 0.7213 seconds, with memory usage at 117.8948 MB and 186.0962 MB, respectively. While higher sampling rates may marginally improve spectral resolution, the associated computational burden may not always justify the benefits, particularly when spectral differences are negligible.Recognizing that the presented simulations represent single-case scenarios, future research should encompass diverse cases and multiple iterations to comprehensively understand the sampling rate's impact on fault diagnosis accuracy and efficiency.

3.3 Case C: Motor with broken rotor bar at no load

In this study the data obtained from the motor with broken rotor bar at no load condition is studied. As slip at low load condition is very low which means the LSB and RSB are very near to fundamental frequency and their amplitude is very weak compare to the amplitude of fundamental component which decreases the visibility of fault based harmonics. Figure 4 shows the spectrum of the data at no load condition for different sampling frequency. From the plot we can see that at no load it is very difficult predict which spectrum is faulty and which one is healthy as the spectrum of healthy and faulty condition are almost identical. Even if we resampled the original sampling rate the fault harmonics cannot be seen.

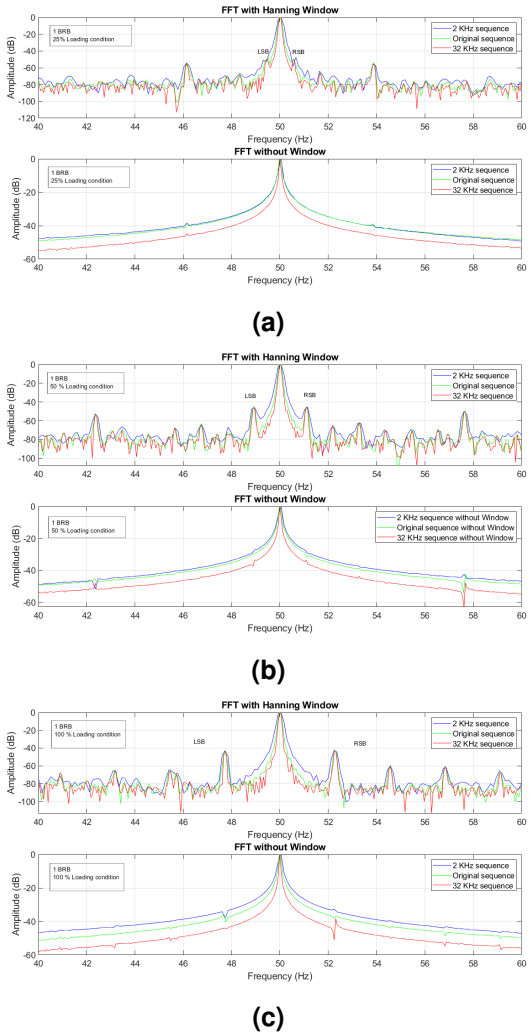

Figure 2: FFT spectrum of original and resampled data signal for motor with 1 BRB with and without Hann window. a) at 25% loading, b) at 50% loading, c) at 100% loading

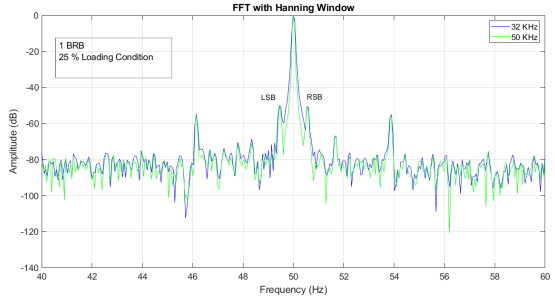

Figure 3: Comparison of FFT spectrum of 32 KHz and 50 KHz data signal for motor with BRB1 at 25% loading condition.

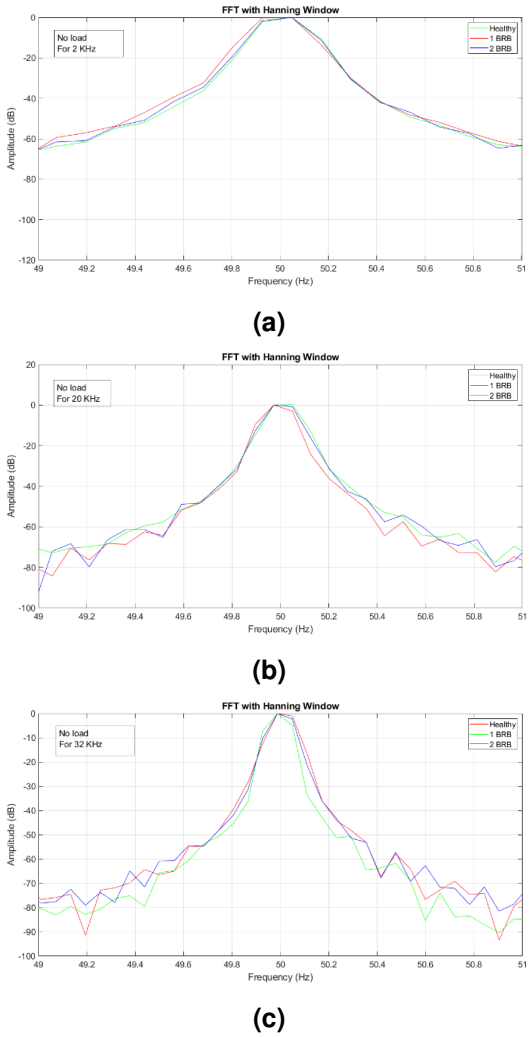

Figure 4: FFT spectrum of the healthy and motor with broken rotor bars at no load for different sampling rates of input signal, a)for 2 KHz, b) for 20 KHz, c) for 32 KHz

4. Conclusion

The analysis highlights the significance of sampling rates in signal spectrum-based fault diagnosis of induction machines. The study demonstrates that changing sampling rates can affect the visibility and sharpness of fault-related harmonics in the FFT spectrum. The use of Hann window functions proves effective in mitigating spectral leakage issues. The results emphasize the need for a careful selection of sampling rates based on fault characteristics and computational considerations. Higher sampling rates may not necessarily improve fault detection and can lead to increased computational complexity without significant benefits. In conclusion, the research provides valuable insights into optimizing sampling rates for fault diagnosis in induction machines,

contributing to the development of efficient and reliable diagnostic systems for industrial applications.

Acknowledgments

This work was supported by the Department of Electrical Engineering and Automation, Aalto University, Finland under the project Capacity Enhancement of Electrical Equipment Condition Monitoring and Fault Diagnostics (CEEECoM).

References

[1] J. Pyrhonen, T. Jokinen, and V. Hrabovcova, *Design of rotating electrical machines*. John Wiley & Sons, 2013.

[2] A. Bellini, F. Filippetti, C. Tassoni, and G.-A. Capolino, "Advances in diagnostic techniques for induction machines," *IEEE Transactions on industrial electronics*, vol. 55, no. 12, pp. 4109–4126, 2008.

[3] B. Asad, H. A. Raja, T. Vaimann, A. Kallaste, R. Pomarnacki, and V. K. Hyunh, "A current spectrum-based algorithm for fault detection of electrical machines using low-power data acquisition devices," *Electronics*, vol. 12, no. 7, p. 1746, 2023.

[4] X. Liang, M. Z. Ali, and H. Zhang, "Induction motors fault diagnosis using finite element method: A review," *IEEE Transactions on Industry Applications*, vol. 56, no. 2, pp. 1205–1217, 2019.

[5] R. de Jesus Romero-Troncoso, "Multirate signal processing to improve fft-based analysis for detecting faults in induction motors," *IEEE Transactions on industrial informatics*, vol. 13, no. 3, pp. 1291–1300, 2016.

[6] B. Asad, T. Vaimann, A. Kallaste, A. Rassõlkin, A. Belahcen, and M. N. Iqbal, "Improving legibility of motor current spectrum for broken rotor bars fault diagnostics," *Electrical, Control and Communication Engineering*, vol. 15, no. 1, pp. 1–8, 2019.

[7] B. Asad, T. Vaimann, A. Kallaste, and A. Belahcen, "Harmonic spectrum analysis of induction motor with broken rotor bar fault," in *2018 IEEE 59th International Scientific Conference on Power and Electrical Engineering of Riga Technical University (RTUCON)*, pp. 1–7, IEEE, 2018.

[8] J. Milimonfared, H. M. Kelk, S. Nandi, A. D. Minassians, and H. A. Toliyat, "A novel approach for broken-rotor-bar detection in cage induction motors," *IEEE Transactions on Industry Applications*, vol. 35, no. 5, pp. 1000–1006, 1999.

[9] V. K. Madisetti and I. T. Young, *The Digital Signal Processing Handbook-3 Volume Set*. CRC press, 2018.

APPENDIX B: PLAGIARISM REPORT

Signal Spectrum Based Condition Monitoring of Electrical Machines Based on Low Sampling Rate

ORIGINALITY REPORT

15%
SIMILARITY INDEX

PRIMARY SOURCES

1	Bilal Asad, Toomas Vaimann, Ants Kallaste, Anton Rassõlkin, Anouar Belahcen, M. Naveed Iqbal. "Improving Legibility of Motor Current Spectrum for Broken Rotor Bars Fault Diagnostics", Electrical, Control and Communication Engineering, 2019 Crossref	227 words — 1%
2	mdpi-res.com Internet	194 words — 1%
3	aaltodoc.aalto.fi Internet	186 words — 1%
4	Rene de Jesus Romero-Troncoso. "Multirate Signal Processing to Improve FFT-Based Analysis for Detecting Faults in Induction Motors", IEEE Transactions on Industrial Informatics, 2017 Crossref	173 words — 1%
5	www.mdpi.com Internet	168 words — 1%
6	www.scilit.net Internet	149 words — 1%
7	www.researchgate.net Internet	119 words — 1%

8	itslearningakarmazyan.files.wordpress.com Internet	75 words —	< 1%
9	psecommunity.org Internet	73 words —	< 1%
10	Peter Tavner, Li Ran, Jim Penman, Howard Sedding. "Introduction to condition monitoring", Institution of Engineering and Technology (IET), 2008 Crossref	67 words —	< 1%
11	hal.archives-ouvertes.fr Internet	49 words —	< 1%
12	research.aalto.fi Internet	49 words —	< 1%
13	core.ac.uk Internet	46 words —	< 1%
14	Belahcen, Anouar, Antero Arkkio, and Javier Martinez. "Broken bar indicators for cage induction motors and their relationship with the number of consecutive broken bars", IET Electric Power Applications, 2013. Crossref	39 words —	< 1%
15	Hadi Ashraf Raja, Karolina Kudelina, Bilal Asad, Toomas Vaimann, Ants Kallaste, Anton Rassõlkin, Huynh Van Khang. "Signal Spectrum-Based Machine Learning Approach for Fault Prediction and Maintenance of Electrical Machines", Energies, 2022 Crossref	32 words —	< 1%
16	fastercapital.com Internet	31 words —	< 1%
17	dokumen.pub		

Internet

28 words — < 1%

18 Siddique Akbar, Toomas Vaimann, Bilal Asad, Ants Kallaste, Muhammad Usman Sardar, Karolina Kudelina. "State-of-the-Art Techniques for Fault Diagnosis in Electrical Machines: Advancements and Future Directions", Energies, 2023

Crossref

27 words — < 1%

19 M. Eltabach, A. Charara, I. Zein. "A Comparison of External and Internal Methods of Signal Spectral Analysis for Broken Rotor Bars Detection in Induction Motors", IEEE Transactions on Industrial Electronics, 2004

Crossref

25 words — < 1%

20 digi.lib.ttu.ee

Internet

24 words — < 1%

21 Bilal Asad, Toomas Vaimann, Anouar Belahcen, Ants Kallaste, Anton Rassõlkin, Muhammad Naveed Iqbal. "Broken rotor bar fault detection of the grid and inverter-fed induction motor by effective attenuation of the fundamental component", IET Electric Power Applications, 2019

Crossref

23 words — < 1%

22 J.A. Antonino-Daviu. "Validation of a New Method for the Diagnosis of Rotor Bar Failures via Wavelet Transform in Industrial Induction Machines", IEEE Transactions on Industry Applications, 7/2006

Crossref

22 words — < 1%

23 Karolina Kudelina, Bilal Asad, Toomas Vaimann, Anton Rassõlkin, Ants Kallaste, Huynh Van Khang. "Methods of Condition Monitoring and Fault Detection for Electrical Machines", Energies, 2021

Crossref

22 words — < 1%

24	Choi, Seungdeog, Bilal Akin, and Ph D. "Implementation of Motor Current Signature An.alysis Fault Diagnosis Based on Digital Signal Processors", Electric Machines Modeling Condition Monitoring and Fault Diagnosis, 2012. Crossref	20 words — < 1%
25	hdl.handle.net Internet	17 words — < 1%
26	etd.adm.unipi.it Internet	15 words — < 1%
27	Jawad Faiz. "Signature Analysis of Electrical and Mechanical Signals for Diagnosis of Broken Rotor Bars in an Induction Motor", Electromagnetics, 11/2007 Crossref	14 words — < 1%
28	Parlos, A.G.. "Sensorless detection of mechanical faults in electromechanical systems", Mechatronics, 200405 Crossref	14 words — < 1%
29	slideplayer.com Internet	14 words — < 1%
30	theses.hal.science Internet	14 words — < 1%
31	Bilal Asad, Toomas Vaimann, Anouar Belahcen, Ants Kallaste. "Broken Rotor Bar Fault Diagnostic of Inverter Fed Induction Motor Using FFT, Hilbert and Park's Vector Approach", 2018 XIII International Conference on Electrical Machines (ICEM), 2018 Crossref	13 words — < 1%

32	Shafi Md Kawsar Zaman, Xiaodong Liang, Weixing Li. "Fault Diagnosis for Variable Frequency Drive-Fed Induction Motors Using Wavelet Packet Decomposition and Greedy-Gradient Max-Cut Learning", IEEE Access, 2021 Crossref	13 words — < 1%
33	link.springer.com Internet	13 words — < 1%
34	Bilal Asad, Toomas Vaimann, Anouar Belahcen, Ants Kallaste, Anton Rassõlkin, M. Naveed Iqbal. "The Cluster Computation-Based Hybrid FEM–Analytical Model of Induction Motor for Fault Diagnostics", Applied Sciences, 2020 Crossref	12 words — < 1%
35	H. Rodriguez Cortes. "Dynamical models for fault detection in squirrel cage induction motors", International Journal of Critical Infrastructures, 2007 Crossref	12 words — < 1%
36	Tavner, P.J.. "Review of condition monitoring of rotating electrical machines", IET Electric Power Applications, 2008. Crossref	12 words — < 1%
37	repository.tudelft.nl Internet	12 words — < 1%
38	Jesus Joaquin Yanez-Borjas, David Camarena-Martinez, Miguel Alfonso Vasquez-Barrera, Rene J. Romero-Troncoso et al. "Experimental Validation of the Broken Rotor Bar Fault Evolution in Line-Fed Induction Motors", 2018 IEEE International Autumn Meeting on Power, Electronics and Computing (ROPEC), 2018 Crossref	11 words — < 1%

39	inscricao.faculdadeitop.edu.br Internet	11 words — < 1%
40	LIANG, B.. "ASYMMETRICAL STATOR AND ROTOR FAULTY DETECTION USING VIBRATION, PHASE CURRENT AND TRANSIENT SPEED ANALYSIS", Mechanical Systems and Signal Processing, 200307 Crossref	10 words — < 1%
41	Manuel Ugidos Guerrero. "Statistical Methods Development for the Multiomic Systems Biology", Universitat Politecnica de Valencia, 2023 Crossref Posted Content	10 words — < 1%
42	O. Didier, E. Ternisien, O. Caspary, H. Razik, H. Henao, A. Yazidi, G.-A. Capolino. "Rotor fault detection using the instantaneous power signature", 2004 IEEE International Conference on Industrial Technology, 2004. IEEE ICIT '04., 2004 Crossref	10 words — < 1%
43	Sasi, A.Y.B.. "A validated model for the prediction of rotor bar failure in squirrel-cage motors using instantaneous angular speed", Mechanical Systems and Signal Processing, 200610 Crossref	10 words — < 1%
44	moam.info Internet	10 words — < 1%
45	www.coursehero.com Internet	10 words — < 1%
46	Didier, G.. "A new approach to detect broken rotor bars in induction machines by current spectrum analysis", Mechanical Systems and Signal Processing, 200702 Crossref	9 words — < 1%

47 N. Arthur, J. Penman. "Induction machine condition monitoring with higher order spectra", IEEE Transactions on Industrial Electronics, 2000
Crossref
9 words — < 1%

48 www.diagnostyka.net.pl
Internet
9 words — < 1%

49 B. Asad, T. Vaimann, A. Belahcen, A. Kallaste, A. Rassolkin, H. Heidari. "The Low Voltage Start-up Test of Induction Motor for the Detection of Broken Bars", 2020 International Conference on Electrical Machines (ICEM), 2020
Crossref
8 words — < 1%

50 Bilal Asad, Hans Tiismus, Toomas Vaimann, Anouar Belahcen, Ants Kallaste, Anton Rassõlkin, Payam Shams Ghafarokhi. "Sliding Mean Value Subtraction-Based DC Drift Correction of B-H Curve for 3D-Printed Magnetic Materials", Energies, 2021
Crossref
8 words — < 1%

51 COMPEL: The International Journal for Computation and Mathematics in Electrical and Electronic Engineering, Volume 22, Issue 4 (2006-09-19)
Publications
8 words — < 1%

52 H.-J. Woe. "Statistical analysis on a case study of load effect on PSD technique for induction motor broken rotor bar fault detection", 4th IEEE International Symposium on Diagnostics for Electric Machines Power Electronics and Drives 2003 SDEMPED 2003 DEMPED-03, 2003
Crossref
8 words — < 1%

53 Jawad Faiz, Bashir Mahdi Ebrahimi. "Determination of Number of Broken Rotor Bars and Static Eccentricity Degree in Induction Motor under Mixed Fault", Electromagnetics, 2008
8 words — < 1%

Crossref

54	R.J. Romero-Troncoso, A. Garcia-Perez, D. Morinigo-Sotelo, O. Duque-Perez, R.A. Osornio-Rios, M.A. Ibarra-Manzano. "Rotor unbalance and broken rotor bar detection in inverter-fed induction motors at start-up and steady-state regimes by high-resolution spectral analysis", Electric Power Systems Research, 2016 Crossref	8 words — < 1%
55	Rodriguez, P.V.J.. "A simplified scheme for induction motor condition monitoring", Mechanical Systems and Signal Processing, 200807 Crossref	8 words — < 1%
56	Weidong Li. "Induction motor fault detection using vibration and stator current methods", Insight - Non-Destructive Testing and Condition Monitoring, 08/2004 Crossref	8 words — < 1%
57	Zhengping Zhang, Zhen Ren, Wenying Huang. "A novel detection method of motor broken rotor bars based on wavelet ridge", IEEE Transactions on Energy Conversion, 2003 Crossref	8 words — < 1%
58	citeseerx.ist.psu.edu Internet	8 words — < 1%
59	doczz.net Internet	8 words — < 1%
60	epdf.pub Internet	8 words — < 1%
61	pdfkiwi.com Internet	8 words — < 1%

62	ruor.uottawa.ca Internet	8 words — < 1%
63	www.treccani.it Internet	8 words — < 1%
64	B. Hafez Bahgat, Enas A. Elhay, Mahmoud M. Elkholy. "Advanced fault detection technique of three phase induction motor: comprehensive review", Discover Electronics, 2024 Crossref	7 words — < 1%
65	Fundamentals of Music Processing, 2015. Crossref	7 words — < 1%
66	H. Douglas, P. Pillay, A.K. Ziarani. "A New Algorithm for Transient Motor Current Signature Analysis Using Wavelets", IEEE Transactions on Industry Applications, 2004 Crossref	7 words — < 1%
67	Wang, F.. "Continuous and real-time data acquisition system for superconducting tokamaks HT-7 and TRIAM-1M", Fusion Engineering and Design, 200602 Crossref	7 words — < 1%
68	A.R. Sadeghian. "Induction motor mechanical fault online diagnosis with the application of artificial neural network", APEC 2001 Sixteenth Annual IEEE Applied Power Electronics Conference and Exposition (Cat No 01CH37181) APEC-01, 2001 Crossref	6 words — < 1%
69	A.R. Sadeghian. "Signature analysis of induction motor mechanical faults by wavelet packet decomposition", APEC 2001 Sixteenth Annual IEEE Applied	6 words — < 1%

Power Electronics Conference and Exposition (Cat No 01CH37181) APEC-01, 2001
Crossref

70 Mingyue Zhu, Jing Zhang, Shaohua Hu, Xingwen Yi, Bo Xu, Meng Xiang, Kun Qiu. "Complexity Reduction With a Simplified MIMO Volterra Filter for PDM-Twin-SSB PAM-4 Transmission", Journal of Lightwave Technology, 2020 — 6 words — < 1%
Crossref

71 Randy Supangat, Jason Grieger, Nesimi Ertugrul, Wen L. Soong, Douglas A. Gray, Colin Hansen. "Detection of Broken Rotor Bar Faults and Effects of Loading in Induction Motors during Rundown", 2007 IEEE International Electric Machines & Drives Conference, 2007 — 6 words — < 1%
Crossref

72 doi.org — 6 words — < 1%
Internet

EXCLUDE QUOTES	ON	EXCLUDE SOURCES	OFF
EXCLUDE BIBLIOGRAPHY	ON	EXCLUDE MATCHES	OFF